122.84, 127.12, 127.76, 128.42, 130.88, 136.98, 146.98, 147.72, 170.56; IR (KBr): 1242 (S=O), 1736 (C=O) cm^{-1}; MS (EI) *m/z* 452 (M^+); HRMS (EI): calcd for $C_{22}H_{28}O_8S$: 452.1505 (M^+), found: 452.1512; $[\alpha]_D^{25}$ +2.76 (*c* 1.40, $CHCl_3$).

*4.1.3.5. (R)-4-(4-Benzyloxy-3-hydeorxybenzyl)dihydrofuran-2-one (**11**).* To a stirred solution of **10** (993 mg, 2.19 mmol) in DMSO (20 mL) was added KCN (150 mg, 2.19 mmol), and the resulting mixture was heated at 90 °C for 3 h. After cooling, the reaction was quenched with H_2O (20 mL), and the aqueous mixture was extracted with Et_2O/AcOEt (1:1, 20 mL × 3). The organic extracts were combined, dried over $MgSO_4$, and evaporated to give cyanide, which was used directly in the next step. To a stirred solution of cyanide obtained above in THF–H_2O (3:1, 8 mL) was added $LiOH \cdot H_2O$ (91.9 mg, 2.19 mmol), and the reaction mixture was stirred at room temperature for 24 h. The reaction mixture was diluted with H_2O (10 mL), and the aqueous mixture was extracted with Et_2O (20 mL × 3). The organic extracts were combined, dried over $MgSO_4$, and evaporated to give alcohol, which was used directly in the next step. The alcohol obtained above was dissolved in 10% NaOH (aq) (10 mL), and the mixture was refluxed for 5 h. After cooling, 10% HCl (aq) (20 mL) and THF (20 mL) were added to the reaction mixture, and the resulting solution was stirred at room temperature for 50 h. The aqueous reaction mixture was extracted with Et_2O (30 mL × 3), and the organic extracts were combined, dried over $MgSO_4$, and evaporated to give a residue, which was chromatographed on silica gel (20 g, hexane:acetone = 3:1) to give **11** (479 mg, 73% in 4 steps) as a colorless solid: ^1H NMR (300 MHz, $CDCl_3$) δ: 2.17–2.32 (1H, m), 2.52–2.69 (3H, m), 2.74–2.86 (1H, m), 3.91–4.05 (1H, m), 4.30–4.36 (1H, m), 5.09 (2H, s), 5.67 (1H, br), 6.59–6.89 (3H, m), 7.36–7.85 (5H, m); ^{13}C NMR (75 MHz, $CDCl_3$) δ: 34.25, 37.22, 38.41, 71.22, 72.63, 112.26, 114.78, 120.04, 127.69, 128.32, 128.61, 131.72, 136.09, 144.50, 145.89, 176.68; IR (KBr): 1647 (C=O), 3445 (OH) cm^{-1}; MS (EI) *m/z* 298 (M^+); HRMS (EI): calcd for $C_{18}H_{18}O_4$: 298.1205 (M^+), found: 298.1204; $[\alpha]_D^{26}$ +5.6 (*c* 0.13, $CHCl_3$); mp: 137–139 °C.

*4.1.3.6. (R)-4-(4-Benzyloxy-3-methoxybenzyl)dihydrofuran-2-one (**12a**).* To a stirred solution of **11** (330 mg, 1.1 mmol) in acetone (15 mL) were added K_2CO_3 (168 mg, 1.2 mmol) and MeI (0.41 mL, 6.6 mmol), and the reaction mixture was refluxed for 24 h. After cooling, the insoluble materials were filtered, and the filtrate was evaporated to give a residue, which was chromatographed on silica gel (15 g, hexane:acetone = 4:1) to give **12a** (304 mg, 88%) as a colorless oil: ^1H NMR (300 MHz, $CDCl_3$) δ: 2.17 (2H, s), 2.24–2.30 (1H, m), 3.88 (3H, s), 4.03–4.05 (1H, m), 4.30–4.35 (1H, m), 5.13 (2H, s), 6.61–6.64 (2H, m), 6.81–6.83 (1H, m), 7.27–7.45 (5H, m); ^{13}C NMR (75 MHz, $CDCl_3$) δ: 34.29, 37.30, 38.64, 56.06, 71.11, 72.60, 112.32, 114.23, 120.52, 127.12, 127.72, 128.40, 131.25, 136.96, 146.91, 149.66, 176.65; IR (neat): 1654 (C=C), 1774 (C=O) cm^{-1}; MS (EI) *m/z* 312 (M^+); HRMS (EI): calcd for $C_{19}H_{20}O_4$: 312.1362 (M^+), found: 312.1380; $[\alpha]_D^{25}$ +4.9 (*c* 0.95, $CHCl_3$).

*4.1.3.7. (R)-4-(4-Benzyloxy-3-ethoxybenzyl)dihydrofuran-2-one (**12b**).* By the procedure similar to preparation of **12a**, **12b** was prepared from **11** and EtI (84%) as a pale yellow oil: ^1H NMR (300 MHz, $CDCl_3$) δ: 1.44 (3H, t, *J* = 4.4 Hz), 2.28 (1H, dd, *J* = 17.3, 6.9 Hz), 2.60 (1H, dd, *J* = 17.3, 8.0 Hz), 2.67–2.84 (3H, m), 4.02–4.13 (3H, m), 4.32 (1H, dd, *J* = 9.1, 6.9 Hz), 5.12 (2H, s), 6.60–6.69 (2H, m), 6.84 (1H, d, *J* = 8.2 Hz), 7.30–7.77 (5H, m); ^{13}C NMR (75 MHz, $CDCl_3$) δ: 15.03, 34.29, 37.31, 38.61, 64.74, 71.37, 72.62, 114.29, 115.22, 120.73, 127.08, 127.63, 128.34, 131.46, 137.20, 147.33, 149.18, 176.67; IR (neat): 1507 (C=C), 1772 cm^{-1} (C=O); MS (EI) *m/z* 326 (M^+); HRMS (EI): calcd for $C_{20}H_{22}O_4$: 326.1518 (M^+), found: 326.1523; $[\alpha]_D^{26}$ +3.4 (*c* 1.78, $CHCl_3$).

*4.1.3.8. (R)-4-(4-Benzyloxy-3-propoxybenzyl)dihydrofuran-2-one (**12c**).* By the procedure similar to preparation of **12a**, **12c** was prepared from **11** and *n*-PrBr (87%) as a colorless oil: ^1H NMR (600 MHz, $CDCl_3$) δ: 1.04 (3H, t, *J* = 7.0 Hz), 1.84 (2H, sextet, *J* = 7.0 Hz), 2.26 (1H, dd, *J* = 17.5, 7.0 Hz), 2.57 (1H, dd, *J* = 17.5, 8.1 Hz), 2.64–2.71 (2H, m), 2.74–2.83 (1H, m), 3.96 (2H, t, *J* = 7.0 Hz), 4.00 (1H, dd, *J* = 9.2, 5.9 Hz), 4.30 (1H, dd, *J* = 9.2, 7.0 Hz), 5.09 (2H, s), 6.60 (1H, d, *J* = 8.1 Hz), 6.67 (1H, s), 6.82 (1H, d, *J* = 8.1 Hz), 7.27–7.42 (5H, m); ^{13}C NMR (100 MHz, $CDCl_3$) δ: 10.46, 22.55, 34.07, 37.15, 38.43, 70.65, 71.32, 72.55, 114.28, 115.38, 120.69, 127.10, 127.63, 128.34, 131.61, 137.31, 147.37, 149.52, 176.84; IR (neat): 1508 (C=C), 1773 (C=O) cm^{-1}; MS (EI) *m/z* 340 (M^+); HRMS (EI): calcd for 340.1675 (M^+), found: 340.1667; $[\alpha]_D^{26}$ −1.0 (*c* 1.05, $CHCl_3$).

*4.1.3.9. (R)-4-(3,4-Dimethoxybenzyl)dihydrofuran-2-one (**13a**).* To a stirred solution of **12a** (302 mg, 0.97 mmol) in MeOH (5 mL) was added 20% $Pd(OH)_2$ (20 mg), and the resulting suspension was stirred under a hydrogen atmosphere at 1 atm for 15 h. The catalyst was removed by filtration and the filtrate was evaporated to give phenol, which was used directly in the next step. To a stirred solution of the phenol obtained above in acetone (10 mL) were added K_2CO_3 (201.1 mg, 1.46 mmol) and MeI (0.18 mL, 2.92 mmol), and the resulting mixture was refluxed for 19 h. After cooling, the insoluble materials were filtered, and the filtrate was evaporated to give a residue, which was chromatographed on silica gel (10 g, hexane:acetone = 4:1) to give **13a** (130 mg, 55% in 2 steps) as a pale yellow oil: ^1H NMR (300 MHz, $CDCl_3$) δ: 2.33 (1H, dd, *J* = 18.0, 9.3 Hz), 2.61 (1H, dd, *J* = 17.4, 8.1 Hz), 2.70–2.87 (3H, m), 3.87 (3H, s), 3.88 (3H, s), 4.05 (1H, dd, *J* = 9.3, 6.3 Hz), 4.33 (1H, dd, *J* = 9.3, 6.6 Hz), 6.66–6.72 (2H, m), 6.82 (1H, d, *J* = 8.1 Hz); $[\alpha]_D^{24}$ +22.2 (*c* 0.87, $CHCl_3$) (ref. [19], $[\alpha]_D^{25}$ +23.8).

*4.1.3.10. (R)-4-(4-Ethoxy-3-methoxybenzyl)dihydrofuran-2-one (**13b**).* By the procedure similar to preparation of **13a**, **13b** was prepared from **12a** and EtI (55% in 2 steps) as a pale yellow oil: ^1H NMR (300 MHz, $CDCl_3$) δ: 1.46 (3H, t, *J* = 7.1 Hz), 2.29 (1H, dd, *J* = 17.6, 6.9 Hz), 2.63 (1H, dd, *J* = 17.6, 8.0 Hz), 2.71–2.88 (3H, m), 3.86 (3H, s), 4.03 (1H, dd, *J* = 9.1, 6.9 Hz), 4.06 (2H, q, *J* = 7.1 Hz), 4.34 (1H, dd, *J* = 9.1, 6.9 Hz), 6.65–6.68 (2H, m), 6.81 (1H, d, *J* = 8.2 Hz); ^{13}C NMR (75 MHz, $CDCl_3$) δ: 14.92, 34.32, 37.36, 38.65, 55.98, 64.38, 72.63, 112.01, 112.84, 120.56, 130.59, 147.06, 149.26, 176.68; IR (neat): 1514 (C=C), 1778 (C=O) cm^{-1}; MS (EI) *m/z* 250 (M^+); HRMS (EI): calcd for $C_{14}H_{18}O_4$: 250.1205 (M^+), found: 250.1192; $[\alpha]_D^{24}$ +4.4 (*c* 1.66, $CHCl_3$).

*4.1.3.11. (R)-4-(3-Ethoxy-4-methoxybenzyl)dihydrofuran-2-one (**13c**).* By the procedure similar to preparation of **13a**, **13c** was prepared from **12b** and MeI (55% in 2 steps) as a pale yellow oil: ^1H NMR (300 MHz, $CDCl_3$) δ: 1.47 (3H, t, *J* = 6.9 Hz), 2.29 (1H, dd *J* = 17.3, 6.6 Hz), 2.61 (1H, dd, *J* = 17.3, 8.0 Hz), 2.67–2.87 (3H, m), 3.86(3H, s), 4.01–4.12 (3H, m), 4.34 (1H, dd, *J* = 9.1, 6.6 Hz), 6.62–6.69 (2H, m), 6.81 (1H, d, *J* = 8.0 Hz); ^{13}C NMR (75 MHz, $CDCl_3$) δ: 14.87, 34.24, 37.31, 38.54, 55.95, 64.35, 72.58, 111.61, 113.24, 120.54, 130.52, 148.01, 148.22, 176.63; IR (neat): 1541 (C=C), 1771 (C=O) cm^{-1}; MS (EI) *m/z* 250 (M^+); HRMS (EI): calcd for $C_{14}H_{18}O_4$: 250.1205 (M^+), found: 250.1207; $[\alpha]_D^{27}$ +4.4 (*c* 1.94, $CHCl_3$).

*4.1.3.12. (R)-4-(3,4-Diethoxybenzyl)dihydrofuran-2-one (**13d**).* By the procedure similar to preparation of **13a**, **13d** was prepared from **12b** and EtI (47% in 2 steps) as a pale yellow oil: ^1H NMR (300 MHz, $CDCl_3$) δ: 1.41–1.47 (6H, m), 2.28 (1H, dd, *J* = 17.3, 6.6 Hz), 2.59 (1H, dd, *J* = 17.3, 8.0 Hz), 2.67–2.86 (3H, m), 4.00–4.11 (5H, m), 4.32 (1H, dd, *J* = 9.3, 6.6 Hz), 6.64–6.67 (2H, m), 6.81 (1H, d, *J* = 8.5 Hz); ^{13}C NMR (75 MHz, $CDCl_3$) δ: 14.97, 34.30, 37.36, 38.61, 64.64, 64.69, 72.65,

113.70, 114.12, 120.78, 130.70, 147.53, 148.72, 176.68; IR (neat): 1507 (C=C), 1771 (C=O) cm^{-1}; MS (EI) *m/z* 264 (M^+); HRMS (EI): calcd for $C_{15}H_{20}O_4$: 264.1362 (M^+), found: 264.1369; $[\alpha]_D^{26}$ +5.4 (*c* 1.29, $CHCl_3$).

*4.1.3.13. (R)-4-(4-Methoxy-3-propoxybenzyl)dihydrofuran-2-one (**13e**).* By the procedure similar to preparation of **13a**, **13e** was prepared from **12c** and MeI (80% in 2 steps) as a pale yellow oil: ^1H NMR (400 MHz, $CDCl_3$) δ: 1.05 (3H, t, *J* = 7.1 Hz), 1.87 (2H, sextet, *J* = 7.1 Hz), 2.29 (1H, dd, *J* = 17.5, 6.8 Hz), 2.60 (1H, dd, *J* = 17.5, 8.1 Hz), 2.65–2.73 (2H, m), 2.77–2.84 (1H, m), 3.85 (1H, s), 3.96 (2H, t, *J* = 7.1 Hz), 4.03 (1H, dd, *J* = 9.3, 6.1 Hz), 4.33 (1H, dd, *J* = 9.3, 7.0 Hz), 6.67 (1H, s), 6.68 (1H, d, *J* = 7.8 Hz), 6.81 (1H, d, *J* = 7.8 Hz); ^{13}C NMR (100 MHz, $CDCl_3$) δ: 10.37, 22.44, 34.15, 37.23, 38.45, 56.00, 70.51, 72,57, 111.89, 113.52, 120.60, 130.67, 148.25, 148.62, 176.86; IR (neat): 1516 (C=C), 1778 (C=O) cm^{-1}; MS (EI) *m/z* 264 (M^+); HRMS(EI): calcd for $C_{15}H_{20}O_4$: 264.1362 (M^+), found: 264.1345; $[\alpha]_D^{26}$ +3.2 (*c* 1.05, $CHCl_3$).

*4.1.3.14. (R)-4-(4-Ethoxy-3-propoxybenzyl)dihydrofuran-2-one (**13f**).* By the procedure similar to preparation of **13a**, **13f** was prepared from **12c** and EtI (77% in 2 steps) as a pale yellow oil: ^1H NMR (400 MHz, $CDCl_3$) δ: 1.05 (3H, t, *J* = 7.0 Hz), 1,42 (3H, t, *J* = 6.8 Hz), 1.87 (2H, sextet, *J* = 7.0 Hz), 2.28 (1H, dd, *J* = 17.5, 7.0 Hz), 2.60 (1H, dd, *J* = 17.5, 8.0 Hz), 2.64–2.72 (2H, m), 2.74–2.85 (1H, m), 3.94 (2H, t, *J* = 7.0 Hz), 4.01–4.09 (3H, m), 4.32 (1H, dd, *J* = 9.1, 6.9 Hz), 6.64 (1H, s), 6.65 (1H, d, *J* = 8.0 Hz), 6.81 (1H, d, *J* = 8.0 Hz); ^{13}C NMR (100 MHz, $CDCl_3$) δ: 10.35, 14.79, 22.50, 34.10, 37.16, 38.38, 64.67, 70.72, 72.56, 114.05, 114.31, 120.78, 130.88, 147.64, 149.09, 176.85; IR (neat): 1510 (C=C), 1774 (C=O) cm^{-1}; MS (EI) *m/z* 278 (M^+); HRMS (EI): calcd for $C_{16}H_{22}O_4$: 278.1518 (M^+), found: 278.1512; $[\alpha]_D^{26}$ +1.2 (*c* 1.05, $CHCl_3$).

*4.1.3.15. (3R,4R)-3-(4-Benzyloxy-3-methoxybenzyl)-4-(3-ethoxy-4-methoxybenzyl)dihydrofuran-2-one (**14a**).* To a stirred solution of **13b** (29.6 mg, 0.12 mmol) in THF (2 mL) were added LiHMDS (1.6 M in THF, 0.12 mL, 0.18 mmol), HMPA (31 μL, 0.18 mmol) at −78 °C, and the resulting solution was stirred at the same temperature for 0.5 h. To the reaction mixture was added a solution of 4-benzyloxy-3-methoxybenzyl bromide [20] (52.3 mg, 0.19 mmol) in THF (2 mL), and allowed to warm to room temperature over 1 h, and then stirred at the same temperature for 20 h. The reaction was quenched with H_2O (4 mL), and the aqueous mixture was extracted with Et_2O (10 mL × 3). The organic extracts were combined, dried over $MgSO_4$, and evaporated to give residue, which was chromatographed on silica gel (10 g, hexane:acetone = 4:1) to give **14a** (25 mg, 44%) as a pale yellow oil: ^1H NMR (300 MHz, $CDCl_3$) δ: 1.44 (3H, t, *J* = 6.9 Hz), 2.46–2.65 (4H, m), 2.91–2.95 (2H, m), 3.79–3.90 (1H, m), 3.84 (6H, s), 4.01 (2H, q, *J* = 6.9 Hz), 4.08–4.20 (1H, m), 5.12 (2H, s), 6.50–6.80 (6H, m), 7.28–7.43 (5H, m); ^{13}C NMR (75 MHz, $CDCl_3$) δ: 14.77, 34.48, 38.02, 41.09, 46.42, 55.90, 64.28, 65.18, 71.03, 71.16, 111.57, 112.85, 113.35, 113.92, 114.02, 120.54, 121.28, 127.17, 127.20, 127.76, 128.46, 130.32, 130.82, 137.06, 147.01, 148.09, 148.26, 149.73, 178.65; IR (neat): 1515 (C=C), 1770 (C=O) cm^{-1}; MS (EI) *m/z* 476 (M^+); HRMS (EI): calcd for $C_{29}H_{32}O_6$: 476.2199 (M^+), found: 476.2197; $[\alpha]_D^{25}$ −16.4 (*c* 0.77, $CHCl_3$).

*4.1.3.16. (3R,4R)-3-(4-Benzyloxy-3-ethoxybenzyl)-4-(3-ethoxy-4-methoxybenzyl)dihydrofuran-2-one (**14b**).* By the procedure similar to preparation of **14a**, **14b** was prepared from **13b** and 4-benzyloxy-3-ethoxybenzyl bromide [21] (59%) as a pale yellow oil: ^1H NMR (300 MHz, $CDCl_3$) δ: 1.34–1.40 (6H, m), 2.36–2.51 (4H, m), 2.81–2.85 (2H, m), 3.71–3.78 (1H, m), 3.75 (3H, s), 3.90–4.05 (5H, m), 5.02 (2H, s), 6.40–6.80 (6H, m), 7.14–7.35 (5H, m); ^{13}C NMR (75 MHz, $CDCl_3$) δ: 14.75, 14.82, 34.43, 37.99, 41.05, 46.39, 55.86, 64.22, 64.47, 71.14, 71.26, 111.51, 113.24, 114.59, 114.97, 120.51, 121.39, 127.11, 127.64, 128.35, 130.31, 130.99, 137.27, 147.33, 148.03, 148.23, 149.24, 178.65; IR (neat): 1507 (C=C), 1771 (C=O) cm^{-1}; MS (EI) *m/z* 490 (M^+); HRMS (EI): calcd for $C_{30}H_{34}O_6$: 490.2355 (M^+), found: 490.2383; $[\alpha]_D^{26}$ −14.8 (*c* 1.46, $CHCl_3$).

*4.1.3.17. (3R,4R)-3-(4-Benzyloxy-3-methoxybenzyl)-4-(4-ethoxy-3-methoxybenzyl)dihydrofuran-2-one (**14c**).* By the procedure similar to preparation of **14a**, **14c** was prepared from **13c** and 4-benzyloxy-3-methoxybenzyl bromide [20] (43%) as a pale yellow oil: ^1H NMR (300 MHz, $CDCl_3$) δ: 1.45 (3H, t, *J* = 6.9 Hz), 2.47–2.63 (4H, m), 2.91–2.95 (2H, m), 3.84 (3H, s), 3.91 (3H, s), 3.91–3.95 (1H, m), 4.09 (2H, q, *J* = 6.9 Hz), 4.03–4.14 (1H, m), 5.16 (2H, s), 6.48–6.96 (6H, m), 7.28–7.45 (5H, m); ^{13}C NMR (75 MHz, $CDCl_3$) δ: 14.90, 34.58, 38.19, 41.13, 46.55, 55.98, 64.35, 65.29, 71.06, 110.88, 112.03, 112.82, 113.89, 113.97, 119.21, 120.44, 121.22, 127.69, 128.40, 130.26, 130.73, 134.03, 136.98, 146.91, 149.61, 178.49; IR (neat): 1261 (C=C), 1770 (C=O) cm^{-1}; MS (EI) *m/z* 476 (M^+); HRMS (EI): calcd for $C_{29}H_{32}O_6$: 476.2199 (M^+), found: 476.2209; $[\alpha]_D^{26}$ −9.0 (*c* 1.75, $CHCl_3$).

*4.1.3.18. (3R,4R)-3-(4-Benzyloxy-3-ethoxybenzyl)-4-(4-ethoxy-3-methoxybenzyl)dihydrofuran-2-one (**14d**).* By the procedure similar to preparation of **14a**, **14d** was prepared from **13c** and 4-benzyloxy-3-ethoxybenzyl bromide [21] (53%) as a pale yellow oil: ^1H NMR (300 MHz, $CDCl_3$) δ: 1.41–1.48 (6H, m), 2.44–2.67 (4H, m), 2.88–2.93 (2H, m), 3.79 (3H, s), 3.80–3.87 (1H, m), 4.02–4.14 (5H, m), 5.11 (2H, s), 6.45–6.96 (6H, m), 7.27–7.45 (5H, m); ^{13}C NMR (75 MHz, $CDCl_3$) δ: 14.62, 14.69, 30.69, 34.27 37.89, 40.87, 46.28, 55.66, 64.12, 64.35, 71.04, 71.12, 111.92, 112.61, 114.52, 114.84, 120.38, 121.31, 127.02, 127.52, 128.23, 130.29, 130.91, 137.17, 146.91, 147.20, 149.10, 178.55; IR (neat): 1515 (C=C), 1771 (C=O) cm^{-1}; MS (EI) *m/z* 490 (M^+); HRMS (EI): calcd for $C_{30}H_{34}O_6$: 490.2355 (M^+), found: 490.2383; $[\alpha]_D^{24}$ −17.9 (*c* 1.14, $CHCl_3$).

*4.1.3.19. (3R,4R)-3-(4-Benzyloxy-3-propoxybenzyl)-4-(3-ethoxy-4-methoxybenzyl)dihydrofuran-2-one (**14e**).* By the procedure similar to preparation of **14a**, **14e** was prepared from **13b** and 4-benzyloxy-3-propoxybenzyl bromide, prepared from 4-benzyl-3-propoxybenzaldehyde [22], (40%) as a pale yellow oil: ^1H NMR (400 MHz, $CDCl_3$) δ: 1.05 (3H, t, *J* = 7.1 Hz), 1.45 (3H, t, *J* = 7.8 Hz), 1.84 (2H, sextet, *J* = 7.1 Hz), 2.46–2.64 (4H, m), 2.86–2.99 (2H, m), 3.80–3.87 (4H, m), 3.94 (2H, t, *J* = 7.1 Hz), 4.00 (2H, q, *J* = 7.8 Hz), 4.06–4.11 (1H, m), 5.10 (2H, s), 6.48–6.82 (6H, m), 7.28–7.44 (5H, m); ^{13}C NMR (100 MHz, $CDCl_3$) δ: 10.47, 14.75, 22.56, 34.47, 38.00, 41.10, 46.40, 55.87, 64.25, 70.53, 71.35, 111.55, 113.29, 114.71, 115.25, 120.52, 121.37, 127.18, 127.57, 127.63, 128.33, 130.35, 131.126, 137.34, 147.40, 148.07, 148.26, 149.57, 178.64; IR (neat): 1514 (C=C), 1771 (C=O) cm^{-1}; MS (EI) *m/z* 504 (M^+); HRMS(EI): calcd for $C_{31}H_{36}O_6$: 504.2512 (M^+), found: 504.2538; $[\alpha]_D^{24}$ −10.7 (*c* 0.75, $CHCl_3$).

*4.1.3.20. (3R,4R)-3-(4-Benzyloxy-3-methoxybenzyl)-4-(3,4-diethoxybenzyl)dihydrofuran-2-one (**14f**).* By the procedure similar to preparation of **14a**, **14f** was prepared from **13d** and 4-benzyloxy-3-methoxybenzyl bromide [20] (48%) as a pale yellow oil: ^1H NMR (300 MHz, $CDCl_3$) δ: 1.41–1.59 (6H, m), 2.43–2.63 (4H, m), 2.91–2.95 (2H, m), 3.82–3.90 (1H, m), 3.85 (3H, s), 3.82–3.89 (1H, m), 3.97–4.12 (5H, m), 5.12 (2H, s), 6.49–6.80 (6H, m), 7.26–7.44 (5H, m); ^{13}C NMR (75 MHz, $CDCl_3$) δ: 14.85, 34.50, 38.07, 41.12, 46.50, 55.96, 64.59, 71.09, 71.21, 112.90, 113.63, 114.06, 114.20, 120.78, 121.33, 127.26, 127.81, 128.51, 130.50, 130.86, 137.12, 147.06, 147.60, 148.77, 149.76, 178.70; IR (neat): 1509 (C=C), 1772 (C=O) cm^{-1}; MS (EI) *m/z* 490 (M^+); HRMS (EI): calcd for $C_{30}H_{34}O_6$: 490.2355 (M^+), found: 490.2388; $[\alpha]_D^{25}$ −13.5 (*c* 0.98, $CHCl_3$).

*4.1.3.21. (3R,4R)-3-(4-Benzyloxy-3-ethoxybenzyl)-4-(3,4-diethoxybenzyl)dihydrofuran-2-one (**14g**).* By the procedure similar to preparation of **14a**, **14g** was prepared from **13d** and 4-benzyloxy-3-ethoxybenzyl bromide [21] (56%) as a pale yellow oil: ^1H NMR

(300 MHz, $CDCl_3$) δ: 1.41–1.44 (9H, m), 2.42–2.60 (4H, m), 3.82–3.86 (1H, m), 4.02–4.13 (7H, m), 5.11 (2H, s), 6.47–6.81 (6H, m), 7.27–7.44 (5H, m); ^{13}C NMR (75 MHz, $CDCl_3$) δ: 14.87, 34.50, 38.09, 41.11, 46.50, 64.60, 71.22, 71.37, 113.63, 114.17, 114.69, 115.08, 120.79, 121.48, 127.21, 127.71, 128.42, 130.53, 131.07, 137.35, 147.41, 147.95, 148.78, 149.32, 178.73; IR (neat): 1514 (C=C), 1770 (C=O) cm^{-1}; MS (EI) m/z 504 (M^+); HRMS (EI): calcd for $C_{31}H_{36}O_6$: 504.2512 (M^+), found: 504.6139; $[\alpha]_D^{25}$ −12.0 (c 0.58, $CHCl_3$).

*4.1.3.22. (3R,4R)-3-(4-Benzyloxy-3-propoxybenzyl)-4-(4-methoxy-3-propoxybenzyl)dihydrofuran-2-one (**14h**).* By the procedure similar to preparation of **14a**, **14h** was prepared from **13e** and 4-benzyloxy-3-propoxybenzyl bromide (49%) as a pale yellow oil: ^1H NMR (400 MHz, $CDCl_3$) δ: 1.02–1.08 (6H, m), 1.82–1.88 (4H, m), 2.45–2.63 (4H, m), 2.85–2.97 (2H, m), 3.83 (3H, s), 3.83–4.60 (6H, m), 5.10 (2H, s), 6.51–6.96 (6H, m), 7.28–7.45 (5H, m); ^{13}C NMR (100 MHz, $CDCl_3$) δ: 10.48, 14.84, 22.56, 34.46, 38.00, 41.07, 46.45, 64.71, 65.15, 70.55, 70.74, 71.18, 71.35, 71.37, 112.76, 114.42, 115.12, 119.34, 120.77, 121.40, 127.13, 127.15, 127.64, 128.34, 128.36, 130.63, 131.13, 137.36, 147.98, 149.58, 178.73; IR (neat): 1514 (C=C), 1771 (C=O) cm^{-1}; MS (EI) m/z 518 (M^+); HRMS(EI): calcd for $C_{32}H_{38}O_6$: 518.2668 (M^+), found: 518.2669; $[\alpha]_D^{25}$ −12.2 (c 0.75, $CHCl_3$).

*4.1.3.23. (3R,4R)-3-(4-Benzyloxy-3-propoxybenzyl)-4-(4-ethoxy-3-propoxybenzyl)dihydrofuran-2-one (**14i**).* By the procedure similar to preparation of **14a**, **14i** was prepared from **13f** and 4-benzyloxy-3-propoxybenzyl bromide (33%) as a pale yellow oil: ^1H NMR (400 MHz, $CDCl_3$) δ: 1.02–1.08 (6H, m), 1.41 (3H, t, J = 7.1 Hz), 1.80–1.91 (4H, m), 2.41–2.63 (4H, m), 2.87–2.94 (2H, m), 3.82–3.96 (5H, m), 4.01 (2H, q, J = 7.1 Hz), 4.05–4.10 (1H, m), 5.10 (2H, s), 6.49–6.96 (6H, m), 7.28–7.45 (5H, m); ^{13}C NMR (100 MHz, $CDCl_3$) δ: 10.50, 22.59, 34.51, 38.05, 41.12, 46.48, 56.00, 65.22, 70.57, 71.40, 111.86, 112.79, 113.63, 114.72, 115.30, 119.36, 120.55, 121.40, 127.16, 127.28, 127.65, 128.36, 130.41, 131.16, 137.37, 147.43, 148.25, 148.58, 149.62, 178.70; IR (neat): 1508 (C=C), 1767 (C=O) cm^{-1}; MS (EI) m/z 532 (M^+); HRMS (EI): calcd for $C_{33}H_{40}O_6$: 532.2825 (M^+), found: 518.2817; $[\alpha]_D^{25}$ −6.3 (c 0.80, $CHCl_3$).

*4.1.3.24. (3R,4R)-4-(3-Ethoxy-4-methoxybenzyl)-3-(4-hydroxy-3-methoxybenzyl)dihydrofuran-2-one (**4g**).* To a stirred solution of **14a** (47.5 mg, 0.10 mmol) in MeOH (5 mL) was added 20% $Pd(OH)_2$ (20 mg), and the resulting suspension was stirred under a hydrogen atmosphere at 1 atm for 20 h. The catalyst was removed by filtration and the filtrate was evaporated to give a residue, which was chromatographed on silica gel (10 g, hexane:acetone = 3:1) to give **4g** (34.1 mg, 89%) as a pale yellow oil: ^1H NMR (300 MHz, $CDCl_3$) δ: 1.45 (3H, t, J = 7.1 Hz), 2.43–2.65 (4H, m), 2.91–2.94 (2H, m), 3.81–3.89 (1H, m), 3.83 (3H, s), 3.84 (3H, s), 4.01 (2H, q, J = 7.1 Hz), 4.12 (1H, dd, J = 9.1, 6.9 Hz), 5.53 (1H, s), 6.47–6.65 (4H, m), 6.69 (1H, d, J = 8.0 Hz), 6.82 (1H, d, J = 8.0 Hz); ^{13}C NMR (75 MHz, $CDCl_3$) δ: 14.80, 30.91, 34.46, 38.09, 40.95, 46.55, 55.83, 55.94, 64.30, 71.27, 99.88, 111.54, 113.26, 114.10, 120.58, 122.08, 129.47, 130.35, 144.52, 146.67, 148.11, 148.33; IR (neat): 1513 (C=C), 1771 (C=O) cm^{-1}; MS (EI) m/z 386 (M^+); HRMS (EI): calcd for $C_{22}H_{26}O_6$: 386.1729 (M^+), found: 386.1693; $[\alpha]_D^{25}$ −17.2 (c 1.44, $CHCl_3$).

*4.1.3.25. (3R,4R)-4-(3-Ethoxy-4-hydroxybenzyl)-3-(3-ethoxy-4-methoxybenzyl)dihydrofuran-2-one (**4h**).* By the procedure similar to preparation of **4g**, **4h** was prepared from **14b** (63%) as a pale yellow oil: ^1H NMR (300 MHz, $CDCl_3$) δ: 1.42–1.47 (6H, m), 2.46–2.63 (4H, m), 2.92 (2H, d, J = 5.8 Hz), 3.81–3.89 (1H, m), 3.84 (3H, s), 3.97–4.12 (5H, m), 5.60 (1H, br), 6.48–6.84 (6H, m); ^{13}C NMR (75 MHz, $CDCl_3$) δ: 14.78, 30.88, 34.39, 38.04, 40.90, 46.53, 55.90, 64.26, 64.39, 71.24, 111.51, 112.37, 113.21, 114.01, 120.55, 121.95, 129.34, 130.35, 144.59, 145.93, 148.08, 148.03, 178.74; IR (neat): 1516 (C=C), 1768 (C=O) cm^{-1}; MS (EI) m/z 400 (M^+); HRMS (EI): calcd for $C_{23}H_{28}O_6$: 400.1886 (M^+), found: 400.1868; $[\alpha]_D^{27}$ −16.9 (c 1.13, $CHCl_3$).

*4.1.3.26. (3R,4R)-4-(4-Ethoxy-3-methoxybenzyl)-3-(4-hydroxy-3-methoxybenzyl)dihydrofuran-2-one (**4i**).* By the procedure similar to preparation of **4g**, **4i** was prepared from **14c** (57%) as a pale yellow oil: ^1H NMR (300 MHz, $CDCl_3$) δ: 1.45 (3H, t, J = 7.1 Hz), 2.44–2.67 (4H, m), 2.93 (2H, d, J = 5.8 Hz), 3.81 (3H, s), 3.82 (3H, s), 3.84–3.99 (1H, m), 4.03–4.15 (1H, m), 4.08 (2H, q, J = 7.1 Hz), 5.30 (1H, br), 6.47–6.66 (4H, m), 6.75 (1H, d, J = 8.0 Hz), 6.82 (1H, d, J = 8.0 Hz); ^{13}C NMR (75 MHz, $CDCl_3$) δ: 14.90, 30.99, 34.53, 38.22, 40.97, 46.63, 55.89, 64.35, 71.31, 111.48, 112.00, 112.71, 114.04, 120.47, 122.01, 129.37, 130.30, 144.39, 146.54, 146.99, 149.18, 178.56; IR (neat): 1749 (C=O), 3648 (OH) cm^{-1}; MS (EI) m/z 386 (M^+); HRMS (EI): calcd for $C_{22}H_{26}O_6$: 386.1729 (M^+), found: 386.1693; $[\alpha]_D^{26}$ −9.5 (c 0.71, $CHCl_3$).

*4.1.3.27. (3R,4R)-4-(3-Ethoxy-4-hydroxybenzyl)-3-(4-ethoxy-3-methoxybenzyl)dihydrofuran-2-one (**4j**).* By the procedure similar to preparation of **4g**, **4j** was prepared from **14d** (63%) as a pale yellow oil: ^1H NMR (300 MHz, $CDCl_3$) δ: 1.39–1.46 (6H, m), 2.41–2.66 (4H, m), 2.91 (2H, d, J = 6.0 Hz), 3.80 (3H, s), 3.81–3.87 (1H, m), 4.00–4.10 (5H, m), 5.64 (1H, br), 6.47–6.65 (4H, m), 6.74 (1H, d, J = 8.2 Hz), 6.82 (1H, d, J = 8.2 Hz); ^{13}C NMR (75 MHz, $CDCl_3$) δ: 14.75, 30.86, 34.35, 38.06, 40.84, 46.54, 55.78, 64.26, 64.37, 71.24, 111.98, 112.38, 112.69, 114.00, 120.52, 121.95, 129.32, 130.38, 144.58, 145.91, 147.07, 149.25; IR (neat): 1771 (C=O), 3548 (OH) cm^{-1}; MS (EI) m/z 400 (M^+); HRMS (EI): calcd for $C_{23}H_{28}O_6$: 400.1886 (M^+), found: 400.1897; $[\alpha]_D^{26}$ −12.4 (c 1.04, $CHCl_3$).

*4.1.3.28. (3R,4R)-4-(3-Ethoxy-4-methoxybenzyl)-3-(4-hydroxy-3-propoxybenzyl)dihydrofuran-2-one (**4k**).* By the procedure similar to preparation of **4g**, **4k** was prepared from **14e** (56%) as a pale yellow oil: ^1H NMR (400 MHz, $CDCl_3$) δ: 1.04 (3H, t, J = 7.4 Hz), 1.45 (3H, t, J = 7.1 Hz), 1.82 (2H, sextet, J = 7.4 Hz), 2.48–2.63 (4H, m), 2.91 (2H, d, J = 5.9 Hz), 3.81–3.88 (4H, m), 3.93 (2H, t, J = 7.4 Hz), 4.02 (2H, q, J = 7.1 Hz), 4.06–4.12 (1H, m), 5.57 (1H, s), 6.48 (1H, s), 6.54 (1H, d, J = 10.2 Hz), 6.60 (1H, d, J = 10.2 Hz), 6.66 (1H,s), 6.75 (1H, d, J = 8.2 Hz), 6.82 (1H, d, J = 8.2 Hz); ^{13}C NMR (100 MHz, $CDCl_3$) δ: 10.43, 14.79, 22.49, 34.41, 38.05, 40.95, 46.54, 55.92, 64.29, 70.32, 71.24, 111.55, 112.43, 113.26, 114.01, 120.57, 121.93, 129.37, 130.37, 144.64, 146.05, 148.12, 148.33, 178.75; IR (neat): 1516 (C=C), 1769 (C=O), 3589 (OH) cm^{-1}; MS (EI) m/z 414 (M^+); HRMS (EI): calcd for $C_{24}H_{30}O_6$: 414.2042 (M^+), found: 414.2046; $[\alpha]_D^{26}$ −10.6 (c 1.10, $CHCl_3$).

*4.1.3.29. (3R,4R)-4-(3,4-Diethoxybenzyl)-3-(4-hydroxy-3-methoxybenzyl)dihydrofuran-2-one (**4l**).* By the procedure similar to preparation of **4g**, **4l** was prepared from **14f** (81%) as a pale yellow oil: ^1H NMR (300 MHz, $CDCl_3$) δ: 1.25–1.45 (6H, m), 2.44–2.66 (4H, m), 2.92 (2H, d, J = 6.0 Hz), 3.83 (3H, s), 3.85–3.89 (1H, m), 3.98–4.13 (5H, m), 5.55 (1H, br), 6.49–6.67 (4H, m), 6.76 (1H, d, J = 7.8 Hz), 6.82 (1H, d, J = 7.8 Hz); ^{13}C NMR (75 MHz, $CDCl_3$) δ: 14.84, 30.91, 34.40, 38.04, 40.94, 46.56, 55.84, 64.58, 71.25, 111.56, 113.60, 114.11, 120.77, 122.10, 129.47, 130.51, 144.51, 146.65, 147.57, 148.78, 178.75; IR (neat): 1766 (C=O), 2978 (OH) cm^{-1}; MS (EI) m/z 400 (M^+); HRMS (EI): calcd for $C_{23}H_{28}O_6$: 400.1886 (M^+), found: 400.1858; $[\alpha]_D^{27}$ −16.0 (c 1.33, $CHCl_3$).

*4.1.3.30. (3R,4R)-4-(3,4-Diethoxybenzyl)-3-(4-hydroxy-3-ethoxybenzyl)dihydrofuran-2-one (**4m**).* By the procedure similar to preparation of **4g**, **4m** was prepared from **14g** (66%) as a pale yellow oil: ^1H NMR (300 MHz, $CDCl_3$) δ: 1.40–1.46 (9H, m), 2.42–2.67 (4H, m), 2.91 (2H, d, J = 5.7 Hz), 3.85 (1H, dd, J = 9.1, 7.4 Hz), 3.97–4.12

(7H, m), 5.59 (1H, br), 6.49–6.66 (4H, m), 6.75 (1H, d, J = 8.0 Hz), 6.82 (1H, d, J = 8.0 Hz); ^{13}C NMR (75 MHz, $CDCl_3$) δ: 14.81, 14.85, 34.39, 38.06, 40.92, 46.58, 64.42, 64.59, 71.27, 112.43, 113.62, 114.05, 114.10, 120.80, 122.00, 129.37, 130.53, 144.61, 145.94, 147.58, 148.80, 178.79; IR (neat): 1516 (C=C), 1761 (C=O) cm^{-1}; MS (EI) m/z 414 (M^+); HRMS (EI): calcd for $C_{24}H_{30}O_6$: 414.2042 (M^+), found: 414.2024; $[\alpha]_D^{25}$ −14.0 (c 0.70, $CHCl_3$).

*4.1.3.31. (3R,4R)-4-(4-Methoxy-3-propoxybenzyl)-3-(4-hydroxy-3-propoxybenzyl)dihydrofuran-2-one (**4n**).* By the procedure similar to preparation of **4g**, **4n** was prepared from **14h** (46%) as a pale yellow oil: ^{1}H NMR (400 MHz, $CDCl_3$) δ: 1.02–1.07 (6H, m), 1.78–1.90 (4H, m), 2.47–2.65 (4H, m), 2.92 (2H, d, J = 5.9 Hz), 3.81 (3H, s), 3.81–3.95 (5H, m), 4.08–4.12 (1H, m), 5.56 (1H, br), 6.50 (1H, s), 6.53 (1H, d, J = 7.9 Hz), 6.60 (1H, d, J = 7.9 Hz), 6.66 (1H, s), 6.75 (1H, d, J = 8.2 Hz), 6.82 (1H, d, J = 8.2 Hz); ^{13}C NMR (100 MHz, $CDCl_3$) δ:10.39, 22.45, 22.47, 34.37, 38.01, 40.91, 46.54, 56.00, 70.29, 70.48, 71.23, 77.21, 111.81, 112.43, 113.53, 114.00, 120.55, 121.90, 129.34, 130.41, 144.61, 146.03, 148.22, 148.58, 178.74; IR (neat): 1516 (C=C), 1767 (C=O), 3422 (OH) cm^{-1}; MS (EI) m/z 428 (M^+); HRMS (EI): calcd for $C_{25}H_{32}O_6$: 428.2199 (M^+), found: 428.2216; $[\alpha]_D^{25}$ −13.7 (c 0.70, $CHCl_3$).

*4.1.3.32. (3R,4R)-4-(4-Ethoxy-3-propoxybenzyl)-3-(4-hydroxy-3-propoxybenzyl)dihydrofuran-2-one (**4o**).* By the procedure similar to preparation of **4g**, **4o** was prepared from **14i** (63%) as a pale yellow oil: ^{1}H NMR (400 MHz, $CDCl_3$) δ: 1.02–1.07 (6H, m), 1.42 (3H, t, J = 7.1 Hz), 1.80–1.86 (4H, m), 2.41–2.63 (4H, m), 2.92 (2H, d, J = 5.9 Hz), 3.83–3.96 (5H, m), 4.01 (2H, q, J = 7.1 Hz), 4.07–4.11 (1H, m), 5.57 (1H, s), 6.51–6.84 (6H, m); ^{13}C NMR (100 MHz, $CDCl_3$) δ: 10.50, 22.59, 34.51, 38.05, 41.12, 46.48, 56.00, 65.22, 70.57, 71.40, 111.86, 112.79, 113.63, 114.72, 115.30, 119.36, 120.55, 121.40, 127.16, 127.28, 127.65, 128.36, 130.41, 131.16, 137.37, 147.43, 148.25, 148.58, 149.62, 178.7010.45, 14.87, 22.50, 22.60, 34.37, 38.04, 40.92, 46.58, 64,76, 70.33, 70.76, 71.26, 100.36, 112.48, 114.02, 114.06, 114.38, 129.37, 130.67, 144.63, 146.04, 147.70, 149.14; IR (neat): 1508 (C=C), 1770 (C=O) cm^{-1}; MS (EI) m/z 442 (M^+); HRMS (EI): calcd for $C_{26}H_{34}O_6$: 442.2355 (M^+), found: 442.2350; $[\alpha]_D^{25}$ −12.9 (c 0.50, $CHCl_3$).

*4.1.4. Effective synthesis of (3R,4R)-4-(3,4-diethoxybenzyl)-3-(4-hydroxy-3-ethoxybenzyl)dihydrofuran-2-one (**4m**)*

*4.1.4.1. 2-(3,4-Diehtoxybenzyl)malonic acid diethyl ester (**17**).* To a stirred solution of (3,4-diehtoxyphenyl)methanol (**16**) [16,23] (733 mg, 3.74 mmol) in CH_2Cl_2 (20 mL) were added NEt_3 (0.67 mL, 4.86 mmol) and MsCl (0.32 mL, 4.11 mmol) at 0 °C, and the reaction mixture was stirred at room temperature for 0.5 h. The reaction was quenched with sat. $NaHCO_3$ (aq) (10 mL), and the organic layer were separated. The aqueous layer was extracted with CH_2Cl_2 (20 mL × 3), and the organic layer and extracts were combined, dried over $MgSO_4$. The solvent was removed under reduced pressure to give a pale yellow oil, which was used directly in the next step. To a stirred solution of diethyl malonate (1.14 ml, 7.48 mmol) in DMF (20 mL) was added NaH (60%, 299 mg, 7.48 mmol) at 0 °C, and the resulting mixture was stirred at room temperature for 1 h. To the solution was added a solution of the oil obtained above in DMF (2 mL) at 0 °C, and the reaction mixture was stirred at room temperature for 25 h. The reaction was quenched with sat. $NaHCO_3$ (aq) (10 mL), and the aqueous mixture was extracted with Et_2O (20 mL × 3). The organic extracts were combined, dried over $MgSO_4$, evaporated to give a pale yellow oil which was chromatographed on silica gel (20 g, hexane:acetone = 15:1) to give **17** (1.10 g, 87% in 2 steps) as a pale yellow oil: ^{1}H NMR (300 MHz, $CDCl_3$) δ: 1.15–1.30 (6H, m), 1.39–1.46 (6H, m), 3.13 (2H, d, J = 8.0 Hz), 3.59 (1H, t, J = 8.0 Hz), 4.01–4.24 (8H, m), 6.68–6.78 (3H, m); ^{13}C NMR (75 MHz, $CDCl_3$) δ: 13.77, 13.83, 14.57, 14.60, 34.06, 41.37, 53.82, 61.11, 64.19, 113.33, 114.09, 120.83, 130.28, 147.28, 148.33, 166.34, 168.64; IR (neat): 1516 (C=C), 1731 (C=O) cm^{-1}; MS (EI) m/z 338 (M^+); HRMS (EI): calcd for $C_{23}H_{28}O_6$: 338.1729 (M^+), found: 338.1766.

*4.1.4.2. (R)-Acetic acid 3-(3,4-diethoxyphenyl-2-hydroxymethylpropyl ester (**18**).* To a stirred solution of **17** (1.43 g, 4.23 mmol) in THF (40 mL) was added $LiAlH_4$ (401 mg, 10.6 mmol) at 0 °C, and the resulting suspension was refluxed for 12 h. The reaction was quenched with 10% NaOH (aq) (20 mL), and the mixture was extracted with AcOEt (20 mL × 5). The organic extracts were combined dried over $MgSO_4$, and the solvent was evaporated to give diol, which was used directly in the next step. To a stirred solution of the diol obtained above in i-Pr_2O–THF (15 mL, 4:1) were added Lipase-PS (323 mg) and vinyl acetate (0.45 ml, 4.85 mmol), and the reaction mixture was stirred at room temperature for 2 h. The catalyst was filtered and the filtrate was evaporated to give residue, which was chromatographed on silica gel (30 g, hexane:acetone = 4:1) to give **18** (669 mg, 53% in 2 steps) as a pale yellow oil. The enantiomeric excess of **18** was determined to be a 98% ee by the Moscher's method [24]. ^{1}H NMR (300 MHz, $CDCl_3$) δ: 1.39–1.44 (6H, m), 2.06 (3H, s), 2.23 (1H, br), 2.49–2.64 (2H, m), 3.45–3.59 (2H, m), 4.01–4.08 (6H, m), 4.15 (1H, dd, J = 11.3, 4.7 Hz), 6.66–6.70 (2H, m), 6.78 (1H, d, J = 8.0 Hz); ^{13}C NMR (75 MHz, $CDCl_3$) δ: 14.88, 20.91, 33.86, 42.53, 62.07, 64.03, 64.55, 64.63, 113.69, 114.52, 121.22, 131.91, 147.23, 148.70, 171.68; IR (neat): 1513 (C=C), 1721 (C=O) cm^{-1}; MS (EI) m/z 296 (M^+); HRMS (EI): calcd for $C_{16}H_{24}O_5$: 296.1624 (M^+), found: 296.1594; $[\alpha]_D^{28}$ +18.8 (c 1.47, $CHCl_3$); 98% ee.

*4.1.4.3. (R)-Acetic acid 3-(3,4-Diethoxyphenyl-2-methanesulfonyloxymethylpropyl ester (**19**).* To a stirred solution of **18** (1.45 g, 4.96 mmol) in CH_2Cl_2 (25 mL) were added MsCl (0.42 ml, 5.45 mmol) and NEt_3 (0.89 ml, 6.45 mmol) at 0 °C, and the reaction mixture was stirred at room temperature for 0.5 h. The reaction was quenched with H_2O (20 mL), and the aqueous mixture was extracted with CH_2Cl_2 (20 mL × 3). The organic extracts were combined dried over $MgSO_4$, and evaporated. The residue was chromatographed on silica gel (40 g, hexane:acetone = 4:1) to give **19** (1.48 g, 79%) as a pale yellow oil: ^{1}H NMR (300 MHz, $CDCl_3$) δ: 1.41–1.46 (6H, m), 2.08 (3H, s), 2.32–2.36 (1H, m), 2.65 (2H, d, J = 7.4 Hz), 2.99 (3H, s), 4.00–4.23 (8H, m), 6.65–6.70 (2H, m), 6.80 (1H, d, J = 8.0 Hz); ^{13}C NMR (75 MHz, $CDCl_3$) δ: 14.85, 20.81, 30.90, 33.49, 37.21, 39.71, 63.02, 64.60, 68.48, 113.70, 114.40, 121.22, 130.36, 147.53, 148.82, 170.78; IR (neat): 1512 (C=C), 1735 (C=O) cm^{-1}; MS (EI) m/z 374 (M^+); HRMS (EI): calcd for $C_{17}H_{26}O_7S$: 374.1399 (M^+), found: 374.1362; $[\alpha]_D^{25}$ +2.1 (c 0.68, $CHCl_3$).

*4.1.4.4. (R)-4-(3,4-Diethoxybenzyl)dihydrofuran-2-one (**13d**) from **19**.* To a stirred solution of **19** (1.12 g, 3.00 mmol) in DMSO (25 mL) was added KCN (205 mg, 3.00 mmol), and the resulting mixture was heated at 90 °C for 3 h. After cooling, the reaction was quenched with H_2O (25 mL), and the aqueous mixture was extracted with Et_2O/AcOEt (1:1, 20 mL × 3). The organic extracts were combined, dried over $MgSO_4$, and evaporated to give cyanide, which was used directly in the next step. To a stirred solution of cyanide obtained above in THF–H_2O (3:1, 12 mL) was added $LiOH \cdot H_2O$ (126 mg, 3.00 mmol), and the reaction mixture was stirred at room temperature for 24 h. The reaction mixture was diluted with H_2O (10 mL), and the aqueous mixture was extracted with Et_2O (20 mL × 3). The organic extracts were combined, dried over $MgSO_4$, and evaporated to give alcohol, which was used directly in the next step. The alcohol obtained above was dissolved in 10% NaOH (aq) (15 mL), and the mixture was refluxed for 5 h. After cooling, 10% HCl (aq) (30 mL) and THF (30 mL) were added to

the reaction mixture, and the resulting solution was stirred at room temperature for 50 h. The aqueous reaction mixture was extracted with Et_2O (30 mL × 3), and the organic extracts were combined, dried over $MgSO_4$, and evaporated to give a residue, which was chromatographed on silica gel (30 g, hexane:acetone = 3:1) to give **13d** (475 mg, 60% in 3 steps) as a pale yellow oil.

4.2. In vitro preferential cytotoxicity

4.2.1. Cells and culture

Human pancreatic cancer cell lines, PANC-1 and CAPAN-1, were maintained in Dulbecco's modified Eagle's medium (DMEM, Nissui Pharmaceutical Co., Ltd., Tokyo, Japan) supplemented with 10% fetal bovine serum (FBS, Gibco BRL Products, Gaithersburg, MD, USA), 0.1% sodium bicarbonate (Nacalai Tesque Inc.), and 1% antibiotic-antimycotic solution (Sigma–Aldrich Inc., St. Louis, MO, USA). Nutrient deprived medium (NDM) contained 265 mg/L $CaCl_2 \cdot 2H_2O$, 0.1 mg/L $Fe(NO_3) \cdot 9H_2O$, 400 mg/L KCl, 200 mg/L $MgSO_4 \cdot 7H_2O$, 6400 mg/L NaCl, 700 mg/L $NaHCO_3$, 125 mg/L NaH_2PO_4, 15 mg/L phenol red, 1 M HEPES buffer (pH 7.4, Wako Pure Chemical Industries, Ltd., Osaka, Japan), and 10 mL MEM vitamin solution (Life Technologies, Inc., Rockville, MD, USA). The final pH was adjusted to 7.4 with 10% $NaHCO_3$. For amino acid supplementation, stock solutions (200 mmol/L L-glutamine solution, MEM amino acids solution, and MEM nonessential amino acids solution; Life Technologies) were added at a concentration of 1%.

4.2.2. Preferential cytotoxicity

Preferential cytotoxicity was determined as previously described [9]. In brief, PANC-1 or CAPAN-1 cells (2×10^4 cells/well) were seeded in 96-well plates (Corning Inc., Corning, NY, USA) and incubated in fresh DMEM at 37 °C under 5% CO_2 and 95% air for 24 h. The cells were washed with Dulbecco's phosphate-buffered saline (PBS, Nissui Pharmaceutical Co., Ltd., Tokyo, Japan) before the medium was replaced with either DMEM or NDM (for CAPAN-1, amino acids-supplimented NDM) containing serial dilutions of the test samples. After 24 h of incubation, the cells were washed with PBS, and 100 μL of DMEM containing 10% WST-8 cell counting kit solution (Dojindo, Kumamoto, Japan) was added to the wells. After 3 h of incubation, the absorbance was measured at 450 nm. Cell viability was calculated from the mean values for three wells using the following equation:

Cell viability (%) = [(Abs(test samples) − Abs(blank))/(Abs((control) − Abs(blank))] × 100

The preferential cytotoxicity was expressed as the concentration at which 50% of cells died preferentially in NDM (PC_{50}).

4.3. In vivo antitumor activity of triethoxy derivative **4m** in nude mice

Five-week-old female BALB/cAJcl-*nu/nu* mice were obtained from CLEA Japan, Inc. (Tokyo, Japan), and 5×10^6 CAPAN-1 cells in 0.3 mL DMEM were s.c. injected into the right side of the back of the animals. Two weeks later, 12 mice bearing tumors around 5 mm in diameter were randomly divided into treatment groups and a vehicle control group. Because (−)-arctigenin (**1**) and triethoxy derivative **4m** are poorly soluble in water, they were first dissolved in DMSO at 10 mg/mL and kept frozen until use. Just before administration, the stock solution was diluted in saline to a final concentration of 250 μg/mL (the final concentration of DMSO in saline is 2.5%). The mice were administered by *i.p.*-injections of 0.2 mL of solution of arctigenin, triethoxy derivative **4m**, or vehicle on 6 days of the week for 4 weeks. The tumor size and body weight were measured weekly and the tumor volume was calculated using the following formula: Tumor volume = $4/3 \times 3.14 \times (L/2 \times W/2 \times W/2)$ where L is the length of the tumor and W is its width. Results are expressed as means ±SD. Statistical comparisons were conducted using Student's t test after ANOVA. The results were considered to be significant when $P < 0.05$.

Acknowledgments

This work was supported in part by grants from the Ministry of Health and Welfare for the Third-Term Comprehensive 10-Year Strategy for Cancer Control and by Grant-in-Aid for Scientific Research (C) (No. 22590098) from Japan Society for the Promotion of Science (JSPS).

Appendix A. Supplementary data

Supplementary data related to this article can be found at http://dx.doi:10.1016/j.ejmech.2012.11.031H.

References

[1] J. Ferlay, H.R. Shin, F. Bray, D. Forman, C. Mathers, D.M. Parkin, GLOBOCAN 2008 v1.2, Cancer Incidence and Mortality Worldwide: IARC CancerBase No. 10 (Internet), International Agency for Research on Cancer, Lyon, France, 2010, Available from:, http://globocan.iarc.fr (accessed 08.05.12).
[2] D. Li, K. Xie, R. Wolff, J.L. Abbruzzese, Pancreatic cancer, Lancet 363 (2004) 1049–1057.
[3] S. Shore, D. Vimalachandran, M.G.T. Raraty, P. Ghaneh, Cancer in the elderly: pancreatic cancer, Surg. Oncol. 13 (2004) 201–210.
[4] H.W. Chung, S.M. Bang, S.W. Park, J.B. Chung, J.K. Kang, J.W. Kim, J.S. Seong, W.J. Lee, S.Y. Song, A prospective randomized study of gemcitabine with doxifluridine versus pacritaxel with doxifluridine in concurrent chemo-radiotherapy for locally advanced pancreatic cancer, Int. J. Radiat. Oncol. 60 (2004) 1494–1501.
[5] C.V. Dang, G.L. Semenza, Oncogenic alteration of metabolism, Trends Biochem. Sci. 24 (1999) 68–72.
[6] M. Kitano, M. Kudo, K. Maekawa, Y. Suetomi, H. Sakamoto, N. Fukuta, R. Nakaoka, T. Kawasaki, Dynamic imaging of pancreatic diseases by contrast enhanced coded phase inversion harmonic ultrasonography, Gut 53 (2004) 854–859.
[7] K. Izuishi, K. Kato, T. Ogura, T. Kinoshita, H. Esumi, Remarkable tolerance of tumor cells to nutrient deprivation: possible new biochemical target for cancer therapy, Cancer Res. 60 (2000) 6201–6207.
[8] (a) H. Esumi, J. Lu, Y. Kurashima, T. Hanaoka, Antitumor activity of pyrvinium pamoate, 6-(dimethylamino)-2-[2-(2,5-dimethyl-1-phenyl-1*H*-pyrrol-3-yl) ethenyl]-1-methyl-quinolinium pamoate salt, showing preferential cytotoxicity during glucose starvation, Cancer Sci. 95 (2004) 685–690;
(b) J. Lu, S. Kunimoto, Y. Yamazaki, M. Kaminishi, H. Esumi, D. Kigamicin, A novel anticancer agent based on a new anti-austerity strategy targeting cancer cells' tolerance to nutrient starvation, Cancer Sci. 95 (2004) 547–552.
[9] S. Awale, J. Lu, S.K. Kalauni, Y. Kurashima, Y. Tezuka, S. Kadota, H. Esumi, Identification of arctigenin as an antitumor agent having the ability to eliminate the tolerance of cancer cells to nutrient starvation, Cancer Res. 66 (2006) 1751–1757.
[10] (a) B. Hausott, H. Greger, B. Marian, Naturally occurring lignans efficiently induce apoptosis in colorectal tumor cells, J. Cancer Res. Clin. Oncol. 129 (2003) 569–576;
(b) T. Matsumoto, K. Hosono-Nishiyama, H. Yamada, Antiproliferative and apoptotic effects of butyrolactone lignans from *Arctium lappa* on leukemic cells, Planta Med. 72 (2006) 276–278;
(c) T. Toyoda, T. Tsukamoto, T. Mizoshita, S. Nishibe, T. Deyama, Y. Takenaka, N. Hirano, H. Tanaka, S. Takasu, H. Ban, T. Kumagai, K. Inada, H. Utsunomiya, M. Tatematsu, Inhibitory effect of nordihydroguaiaretic acid, a plant lignan, on *Helicobacter pylori*-associated gastric carcinogenesis in Mongolian gerbils, Cancer Sci. 98 (2007) 1689–1695.
[11] (a) M. Nose, T. Fujimoto, T. Takeda, S. Nishibe, Y. Ogihara, Structural transformation of lignan compounds in rat gastrointestinal tract, Planta Med. 58 (1992) 520–523;
(b) S. Heinonen, T. Nurmi, K. Liukkonen, K. Poutanen, K. Wähälä, T. Deyama, S. Nishibe, H. Adlercreuta, In vitro metabolism of plant lignans: new precursors of mammalian lignans enterolactone and enterodiol, J. Agr. Food Chem. 49 (2001) 3178–3186;
(c) L.-H. Xie, E.-M. Ahn, T. Akao, A.A. Abdel-Hafez, N. Nakamura, M. Hattori, Transformation of arctiin to estrogenic and antiestrogenic substances by human intestinal bacteria, Chem. Pharm. Bull. 51 (2003) 378–384.
[12] E. Eich, H. Pertz, M. Kaloga, J. Schulz, M.R. Fesen, A. Mazumder, Y. Pommier, (−)-Arctigenin as a lead structure for inhibitors of human immunodeficiency virus type-1 integrase, J. Med. Chem. 39 (1996) 86–95.
[13] M.G. Banwell, S. Chand, G.P. Savage, An enantioselective total synthesis of the stilbenolignan (−)-aiphanol and the determination of its absolute stereochemistry, Tetrahedron: Asymmetry 16 (2005) 1645–1654.

[14] R. Fumeaux, C. Menozzi-Smarrito, A. Stalmach, C. Munari, K. Kraehenbuehl, H. Steiling, A. Crozier, G. Williamson, D. Barron, First synthesis, characterization, and evidence for the presence of hydroxycinnamic acid sulfate and glucuronide conjugates in human biological fluids as a result of coffee consumption, Org. Biomol. Chem. 8 (2010) 5199–5211.
[15] T. Cardinaels, J. Ramaekers, P. Nockemann, K. Driesen, K. Van Hecke, L. Van Meervelt, S. Lei, S. De Feyter, D. Guillon, B. Donnio, K. Binnemans, Imidazo[4,5-f]-1,10-phenanthrolines: versatile ligands for the design of metallomesogens, Chem. Mater. 20 (2008) 1278–1291.
[16] T.C. Daniels, R.E. Lyons, Ethyl esters of triiodophenoxyacetic acids and potassium triiodophenoxyacetate, J. Am. Chem. Soc. 58 (1936) 2646.
[17] M. Lieber, J. Mazzetta, W. Nelson-Rees, M. Kaplan, G. Todaro, Establishment of a continuous tumor-cell line (PANC-1) from a human carcinoma of the exocrine pancreas, Int. J. Cancer 15 (1975) 741–747.
[18] (a) H. Suemizu, M. Monnai, Y. Ohnishi, M. Ito, N. Tamaoki, M. Nakamura, Identification of a key molecular regulator of liver metastasis in human pancreatic carcinoma using a novel quantitative model of metastasis in NOD/SCID/γ_c^{null} (NOG) mice, Int. J. Oncol. 31 (2007) 741–751;
(b) A.P. Kyriazis, A.A. Kyriazis, D.G. Scarpelli, J. Fogh, M.S. Rao, R. Lepera, Human pancreatic adenocarcinoma line Capan-1 in tissue culture and the nude mouse. Morphologic, biologic, and biochemical characteristics, Am. J. Pathol. 106 (1982) 250–260.
[19] S. Koul, B. Singh, S.C. Taneja, G.N. Qazi, New chemo and chemo-enzymatic synthesis of β-benzyl-γ-butyrolactones, Tetrahedron 59 (2003) 3487–3491.
[20] A. Van Oeveren, J.F.G.A. Jansen, B.L. Feringa, Enantioselective synthesis of natural dibenzylbutyrolactone lignans (−)-enterolactone, (−)-hinokinin, (−)-pluviatolide, (−)-enterodiol, and furofuran lignan (−)-eudesmin via tandem conjugate addition tp g-alkoxybutenolides, J. Org. Chem. 59 (1994) 5999–6007.
[21] Aurora Building Blocks, Order Number: A00. 384. 218.
[22] B. Pelcman, J.G.K. Yee, L.F. Macenzie, Y. Zhou, K. Han, Isochromenones as PDE4 and PDE7 inhibitors and their preparation and use in the treatment of inflammation, PCT Int. Appl., 2010076564, 2010.
[23] (a) A. Enoki, M.H. Gold, Degradation of the diarylpropane lignin model compound 1-(3′,4′-diethoxyphenyl)-l,3-dihydroxy-2-(4‴-methoxyphenyl)-propane and derivatives by the basidiomycete *Phanerochaete chrysosporium*, Arch. Microbiol. 132 (1982) 123–130;
(b) V.C. Farmer, M.E.K. Henderson, J.D. Russel, Reduction of certain aromatic acids to aldehydes and alcohols by *Polystictus versicolor*, Biochim. Biophys. Acta 35 (1959) 202–211.
[24] J.A. Dale, S.H. Mosher, Nuclear magnetic resonance enantiomer regents. Configurational correlations via nuclear magnetic resonance chemical shifts of diastereomeric mandelate, *O*-methylmandelate, and α-methoxy-α-trifluoromethylphenylacetate (MTPA) esters, J. Am. Chem. Soc. 95 (1973) 512–519.

OPEN ACCESS Freely available online

PLOS | ONE

Critical Role of H_2O_2 Generated by NOX4 during Cellular Response under Glucose Deprivation

Satoshi Owada[1,2], Yuko Shimoda[1,2], Katsuya Tsuchihara[1,2], Hiroyasu Esumi[1,2]*

1 Department of Integrated Biosciences, Graduate School of Frontier Sciences, The University of Tokyo, Kashiwa, Japan, **2** Cancer Physiology Project, Research Center for Innovative Oncology, National Cancer Center Hospital East, Kashiwa, Japan

Abstract

Glucose is the most efficient energy source, and various cancer cells depend on glycolysis for energy production. For maintenance of survival and proliferation, glucose sensing and adaptation to poor nutritional circumstances must be well organized in cancer cells. While the glucose sensing machinery has been well studied in yeasts, the molecular mechanism of glucose sensing in mammalian cells remains to be elucidated. We have reported glucose deprivation rapidly induces AKT phosphorylation through PI3K activation. We assumed that regulation of AKT is relevant to glucose sensing and further investigated the underlying mechanisms. In this study, AKT phosphorylation under glucose deprivation was inhibited by galactose and fructose, but induced by 2-deoxyglucose (2-DG). Both 2-DG treatment and glucose deprivation were found to induce AKT phosphorylation in HepG2 cells. These findings suggested that glucose transporter may not be involved in the sensing of glucose and induction of AKT phosphorylation, and that downstream metabolic events may have important roles. A variety of metabolic stresses reportedly induce the production of reactive oxygen species (ROS). In the present study, glucose deprivation was found to induce intracellular hydrogen peroxide (H_2O_2) production in HepG2 cells. N-acetylcysteine (NAC), an antioxidant reagent, reduced both the increase in cellular H_2O_2 levels and AKT phosphorylation induced by glucose deprivation. These results strongly suggest that the glucose deprivation-induced increase of H_2O_2 in the cells mediated the AKT phosphorylation. RNA interference of NOX4, but not of NOX5, completely suppressed the glucose deprivation-induced AKT phosphorylation as well as increase of the intracellular levels of ROS, whereas exogenous H_2O_2 could still induce AKT phosphorylation in the NOX4-knockdown cells. In this study, we demonstrated that the ROS generated by NOX4 are involved in the intracellular adaptive responses by recognizing metabolic flux.

Citation: Owada S, Shimoda Y, Tsuchihara K, Esumi H (2013) Critical Role of H_2O_2 Generated by NOX4 during Cellular Response under Glucose Deprivation. PLoS ONE 8(3): e56628. doi:10.1371/journal.pone.0056628

Editor: Junji Yodoi, Institute for Virus Research, Laboratory of Infection and Prevention, Japan

Received October 1, 2012; **Accepted** January 11, 2013; **Published** March 21, 2013

Funding: This work was supported by a Grant for the 3rd Term Comprehensive 10-Year Strategy for Cancer Control from the Ministry of Health, Labour and Welfare Japan [H22-3ji taigann-ippann-033 to HE] (http://www.mhlw.go.jp/english/). No additional external funding received for this study. The funders had no role in study design, data collection and analysis, decision to publish, or preparation of the manuscript.

Competing Interests: The authors have declared that no competing interests exist.

* E-mail: hesumi@ncc.go.jp

Introduction

The supply of nutrients and oxygen is pivotal for cell survival and function, because of the large energy requirements of cells. This need is especially critical during cell proliferation. Proliferation is a process during which the numbers of cells successively double; therefore, the synthesis of nucleic acids, lipids, proteins and sugars is obligatory for successful proliferation. Glucose serves as a carbon source for the synthesis of nucleic acids, non-essential amino acids, lipids, and sugar. The intermediate metabolites in the glycolytic system are indispensable for non-essential amino acid synthesis, and intermediate metabolites and coenzymes in the pentose-5-phosphate pathway are required for the synthesis of nucleic acids and lipids. In addition, glucose is also needed for energy production in all cells.

Because of the pivotal role of glucose in the maintenance of the cellular functions, survival, and proliferation, elaborate mechanisms for detecting glucose availability in the cellular microenvironment exist in cells. The molecular mechanisms involved in the sensing of extracellular glucose concentrations have been extensively studied in yeasts. Yeasts detect the extracellular glucose concentrations using Snf3/Rtg2 (a glucose transporter homolog that has no capability as a transporter). Extracellular glucose causes this sensor to generate an intracellular signal that induces the expressions of several HXT genes encoding hexose transporters. The glucose signal induces HXT gene expression by influencing the function of the Rgt1 transcriptional repressor. In the absence of glucose, Rgt1 is functional and binds to the promoters of the HXT genes, repressing their functions [1,2,3]. In contrast, the biochemical basis of the glucose sensing mechanism in mammalian cells is largely unknown.

Meanwhile, most of human cancer tissues are known to be hypoxic, the hypoxia being caused mainly by a poor and heterogeneous blood supply [4,5,6,7]. Glucose as well as oxygen is supplied to cancer tissues via the blood stream, and we assumed that the glucose supply might be limited in human cancer tissues. In fact, the glucose concentrations in human colon cancer and gastric cancer tissues were found to be significantly lower than those in surrounding non-cancerous tissues [8]. In the cancer cells that exist in such environments, the monitoring of and adaptation to extracellular glucose concentrations are assumed to be important for the survival/proliferation of the tumor cells. We previously reported that AKT phosphorylation is immediately enhanced by the absence of glucose and plays a critical role in

cellular survival under such condition in various cell lines [9,10]. AKT can also be activated in response to a variety of cellular stresses, such as heat shock, ultraviolet light irradiation, ischemia, hypoxia, hyperglycemia, and oxidative stress. AKT is a serine and threonine kinase that mediates cell survival under these aforementioned conditions [11,12,13,14,15].

In the present study, we attempted to elucidate the molecular and biochemical mechanisms involved in the sensing of mammalian cells of the extracellular glucose concentrations, using AKT phosphorylation as an index of the cellular responses to glucose deprivation. We demonstrate the contribution of the H_2O_2 generated by NOX4 in the cellular sensing of and adaptation to poor glucose supply.

Materials and Methods

Cell cultures

Human fibroblasts derived from the subserosa of the stomach used for this study were kindly gifted to us by Dr Atsushi Ochiai (Pathology Division, Research Center for Innovative Oncology, National Cancer Center Hospital East). Human pancreatic cancer cells (PANC-1), human hepatocellular carcinoma cells (HepG2) and human fibroblasts derived from subserosa of the stomach were cultured in DMEM (GIBCO) supplemented with 10% fetal bovine serum (Biowest). All the cells were purchased from ATCC. The glucose-deprived condition was created as described previously [16].

Reagents

2′, 7′- Dichlorodihydrofluorescin diacetate (DCFDA) was purchased from Invitrogen. 3′-O-Acetyl-6′-O-pentafluorobenzenesulfonyl-2′,7′-difluorofluorescein (Bes-H_2O_2), galactose and fructose were purchased from Wako Pure Chemical Industries. N-acetyl-L-cysteine (NAC) and 2-deoxy-D-glucose (2-DG) were purchased from Sigma Aldrich. LY294002 and PP2 were purchased from Calbiochem.

Immunoblot analyses

Cells were homogenized in lysis buffer containing 10% SDS (sodium dodecyl sulfate), 10 mM Tris-HCl (pH 7.5) and 1 mM sodium orthovanadate, as described previously [17], and subjected to SDS-PAGE (SDS polyaclylamide gel electrophoresis). The proteins were transferred to a polyvinylidene fluoride microporous membrane (Millipore). The primary antibodies used were: anti-phospho-AKT Ser-473, anti-phospho-SRC Family Tyr-416, and anti-AKT, all obtained from Cell Signaling Technologies, and anti-actin (sc-1615), and c-SRC antibody (SRC2), obtained from Santa Cruz Biotechnology. The anti-OSSA antibody was a kind gift from Dr. Ryuuichi Sakai, National Cancer Center Research Institute. The following secondary antibodies were purchased from Santa Cruz Biotechnology: goat anti-mouse IgG-HRP, goat anti-rabbit IgG-HRP. The immunoblots were scanned using a CanoScan LiDE60 image scanner (Canon).

siRNA transfection

OSSA, NOX4, NOX5, and non-targeting siRNA were purchased from Invitrogen. For the siRNA experiments, the cells were transfected separately using a non-targeting siRNA or two separate specific siRNAs using Lipofectamine 2000 (Invitrogen).

RT-PCR

Total RNAs were prepared from the cells using ISOGEN (Nippon Gene), and reverse transcription was performed using superscript VILO (Invitrogen). PCR for human NOX family genes was carried out using the following primers: forward 5′-CTCAGCGGAATCAATCAGCTGTG-3′ and reverse 5′-AGAGGAACACGACAATCAGCCTTAG-3′ for Nox4; forward 5′-ATCAAGCGGCCCCCTTTTTTTCAC-3′ and reverse 5′-CTCATTGTCACACTCCTCGACAGC-3′ for Nox5.

Measurement of intracellular ROS levels

The cells were treated under various conditions and then incubated in DMEM or glucose-deprived medium containing 5 μM of DCFDA or 5 μM BES-H_2O_2-Ac at 37°C for 30 min. Then, the cells were detached from the plate with trypsin/EDTA, washed with PBS, resuspended in 500 μL of PBS, and placed on ice, protected from light. The intensity of the fluorescence of each cell was immediately measured using a FACS CANTO (Becton Dickinson) equipped with an argon ion laser (488 nm excitation). Each experiment was conducted in triplicate, and 10,000 cells per sample were measured. The histogram was analyzed using the software program BD FACS DIVA (Becton Dickinson).

Results

AKT activation by glucose deprivation

Within 30 minutes, and still after 3 hours, of transferring the HepG2 cells from ordinary DMEM to glucose-deprived medium, AKT was strongly phosphorylated at Ser 473; furthermore, AKT phosphorylation was significantly inhibited by treatment with LY294002 [18], an inhibitor of PI3K (Fig. 1A). Similarly, PI3K-dependent AKT activation was also observed in the pancreatic PANC-1 cells (Fig. S1) in a previous study [10]. Furthermore, increase of AKT phosphorylation induced by glucose deprivation was also observed in human fibroblasts derived from the subserosa of the stomach (Fig. S2).

To examine how glucose deprivation is recognized in these cells, concentration-dependent AKT activation in response to glucose deprivation was examined. When the HepG2 cells were exposed to media containing less than 1.38 mM of glucose, corresponding to one-quarter of the blood glucose level, AKT activation was clearly observed (Fig. 1B). Similarly, an increase in AKT phosphorylation was also observed in PANC-1 cells cultured in the presence of glucose at concentrations of less than 0.69 mM (Fig. S3). To elucidate the glucose sensing mechanism of the cells, the effect of glucose analogues on the AKT activation in response to glucose deprivation was examined. AKT activation was completely inhibited by the addition of either galactose or fructose at a final concentration of 5.5 mM (Fig. 1C). Similar results were observed in the PANC-1 cells (Fig. S4). These observations indicate that AKT is activated by a decrease of some metabolites of glycolysis or metabolic stress, rather than by the decrease of glucose itself. In yeast, the extracellular glucose concentration is sensed by a glucose transporter [1,2,3]. To examine whether a similar mechanism may also prevail in mammalian cells, the influence of 2-DG [19,20] on the AKT phosphorylation induced by glucose deprivation was examined. As shown in Fig. 1D, AKT phosphorylation in the HepG2 cells in response to glucose deprivation was not inhibited by 2-DG. Rather, AKT phosphorylation was clearly induced by the addition of 5.5 mM 2-DG, even in the presence of glucose. This observation indicates that glucose is not sensed by binding to a receptor or transporter, nor is it sensed by hexokinase, because 2-DG can be phosphorylated as efficiently by mammalian hexokinase as glucose. It is possible that the inhibition of binding of some sensors to glucose, if such an interaction occurs, might evoke the same cellular responses as glucose deprivation.

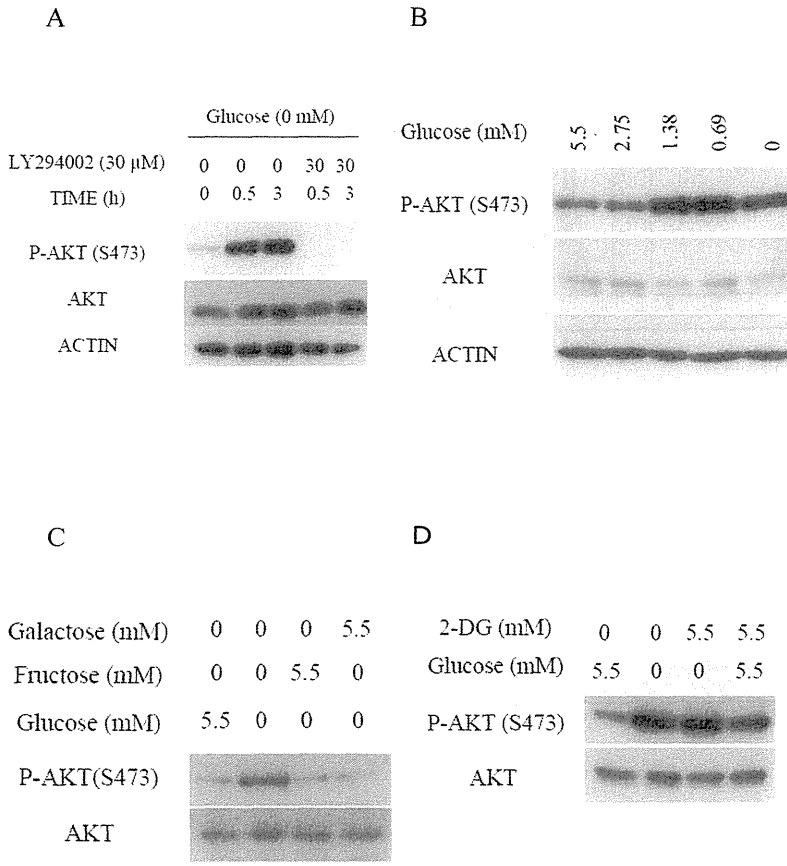

Figure 1. AKT phosphorylation was induced under glucose deprivation. (A) Immunoblotting analyses after incubation of HepG2 cells in the absence or presence of 5.5 mM of glucose and absence or presence of 30 μM of LY294002 for the indicated times. (B) HepG2 cells treated or not treated with various concentrations of glucose for 0.5 h were subjected to immunoblotting. (C) Immunoblotting analyses of HepG2 cells treated or not treated with 5.5 mM of glucose, 5.5 mM of galactose, or 5.5 mM of fructose for 0.5 h. (D) Immunoblotting analyses of HepG2 cells treated or not treated with 5.5 mM of glucose, 5.5 mM of 2-DG, or 5.5 mM of glucose plus 5.5 mM of 2-DG for 0.5 h.
doi:10.1371/journal.pone.0056628.g001

Role of hydrogen peroxide in the activation of AKT in response to glucose deprivation

Since AKT phosphorylation in response to glucose deprivation was attenuated by galactose, we assumed that changes in the metabolism might be the cause of the increase in AKT activation. Reactive oxygen species (ROS) are reportedly produced in cells under metabolic stresses [21,22]. We evaluated the intracellular levels of ROS using dichlorofluorescein diacetate (DCFDA), which measures hydroxyl and peroxyl radicals and other ROS. A significant increase in the intracellular ROS production was observed in the HepG2 cells cultured in glucose-deprived medium treated with DCFDA for 30 minutes (Fig. 2A). 3′-O-acetyl-6′-O-pentafluorobenzenesulfonyl- 2′,7′-difluorofluorescein (BES-H_2O_2) specifically detects an increase in the amounts of hydrogen peroxide (H_2O_2) [23] in cells treated under the same conditions (Fig. 2B). An increase in the production of ROS induced by glucose deprivation was also observed in the PANC-1 cells and human fibroblasts derived from the subserosa of the stomach (Fig. S5,S6). Addition of galactose or fructose completely prevented the H_2O_2 increase (Fig. S7). These results clearly showed that H_2O_2 production is induced by glucose deprivation. To elucidate the causal relationship between H_2O_2 production and AKT phosphorylation, the effect of addition of exogenous H_2O_2 on AKT phosphorylation was examined. Exogenous H_2O_2 addition to the culture medium induced PI3K-dependent AKT phosphorylation in a manner similar to glucose deprivation (Fig. 2C). To confirm the causal relation further, the influence of N-acetylcysteine (NAC), an antioxidant reagent, on the AKT phosphorylation induced in the absence of glucose was examined. The addition of NAC to the culture medium at a final concentration of 12.5 mM markedly reduced the ROS levels even under glucose-deprived conditions (Fig. 2A and 2B). Furthermore, the NAC treatment also suppressed the AKT phosphorylation induced by glucose deprivation (Fig. 2D).

SRC and OSSA are indispensable for AKT phosphorylation induced by glucose deprivation

SRC is involved in an alternate PI3K-activating pathway, and OSSA, a scaffold protein also known as FAM120A, reportedly activates the SRC-PI3K pathway in the presence of oxidative stress [24]. Thus, the involvements of SRC and OSSA in the glucose deprivation-induced phosphorylation of AKT were examined. PP2, a specific SRC family inhibitor [25], clearly inhibited the AKT phosphorylation induced by glucose deprivation (Fig. 3A). PP2 also inhibited AKT phosphorylation induced by exogenous H_2O_2 (Fig. 3B). Consistent with these findings, PP2

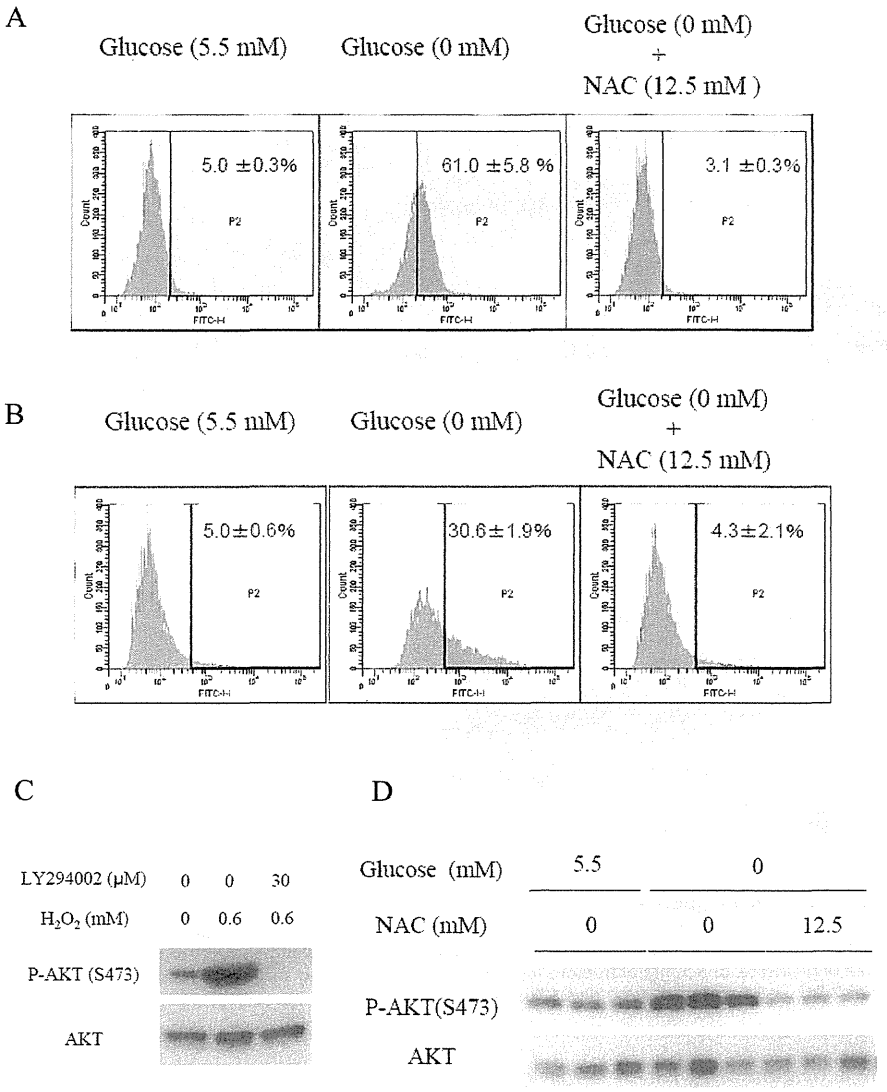

Figure 2. ROS mediates AKT phosphorylation under glucose deprivation. (A)(B)(D) HepG2 cells were cultured in either glucose-containing medium or glucose-deprived medium in the absence or presence of 12.5 mM of NAC for 0.5 h. ROS production was measured using flow cytometry. Cells were stained with (A) 5 μM of DCFDA or (B) 5 μM of BES-H_2O_2. Cells were gated within a range contained in the upper 5% of the total cell count under the glucose replete condition. (D) The AKT phosphorylation level was evaluated by immunoblotting. (C) Addition of H_2O_2 to media containing 5.5 mM of glucose in the absence or presence of 30 μM of LY294002 for 0.5 h, followed by immunoblotting.
doi:10.1371/journal.pone.0056628.g002

also suppressed the phosphorylation of SRC induced by glucose deprivation and exogenous H_2O_2 (Fig. S8). PP2 treatment did not alter the increased ROS levels in HepG2 cells cultured under glucose-deprived conditions (Fig. 3C). Similarly, LY294002 treatment inhibited AKT phosphorylation, but did not alter the ROS production (Fig. 1A, 3C). Suppression of OSSA expression by RNA interference inhibited the AKT phosphorylation induced by glucose deprivation and exogenous H_2O_2 (Fig. 3D, 3E and 3F). Thus, SRC and OSSA were concluded as being mediators of the H_2O_2 signals induced by glucose deprivation that activate the PI3K-AKT axis.

NOX4 knockdown inhibits hydrogen peroxide generation under glucose-deprived conditions

NOX4, one of the members of the NADPH oxidase family, is known to be closely involved in the production of ROS in response to growth factor stimuli [26]. Thus, its involvement also in glucose deprivation-induced AKT phosphorylation was examined. RNA interference selectively reduced the expression of NOX4 in HepG2 cells (Fig. 4A). Increase of intracellular ROS levels by glucose deprivation was suppressed by NOX4 knockdown (Fig. 4B). Consistent with this finding, AKT phosphorylation was also not induced in the NOX4 knockdown cells, while exogenous H_2O_2 clearly induced AKT phosphorylation in the cells (Fig. 4C). Similar results were obtained in the PANC-1 cells (Fig. S9A, B). PANC-1 cells express NOX5 as well as NOX4, however,

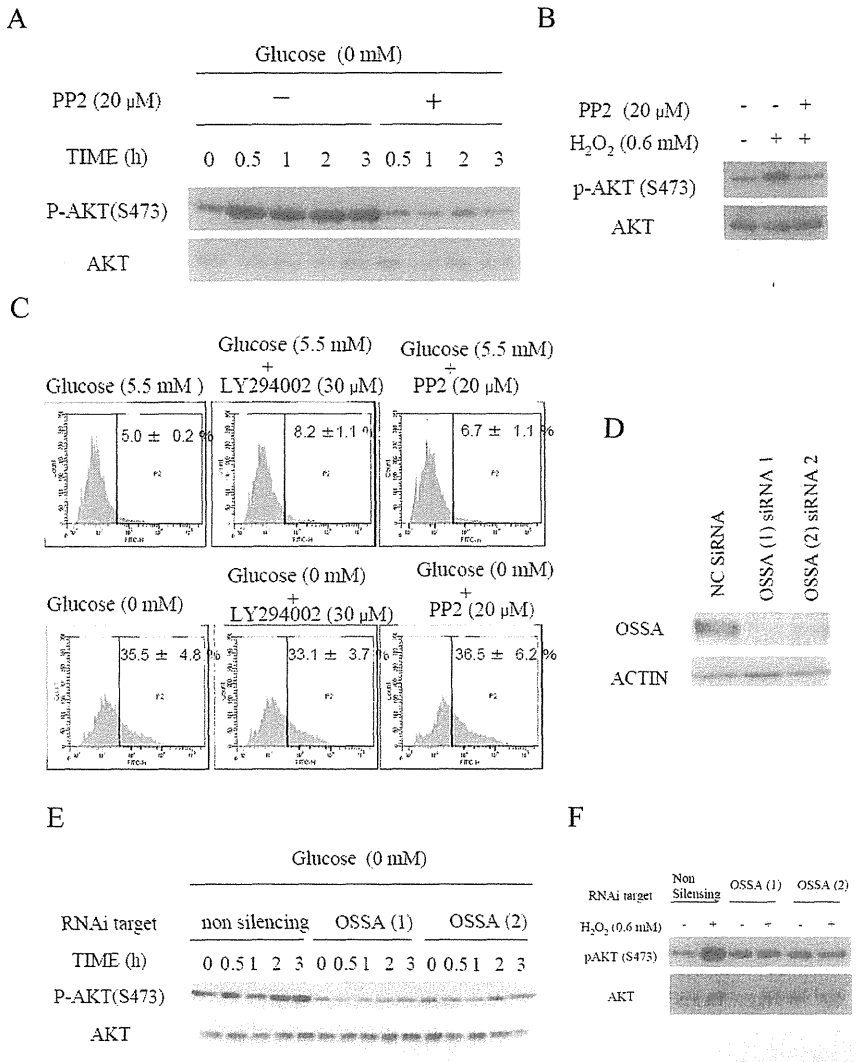

Figure 3. SRC and OSSA are indispensable for the AKT phosphorylation induced by glucose deprivation. (A) Immunoblotting analyses of HepG2 cells in the absence or presence of 5.5 mM of glucose in the and absence or presence of 20 μM of PP2 for the indicated times. (B) Addition of H_2O_2 to the culture medium containing 5.5 mM glucosein the absence or presence of 20 μM of PP2 for 0.5 h, followed by immunoblotting. (C) HepG2 cells were cultured in medium containing or not containing (glucose-deprived) 5.5 mM of glucose in the absence or presence of 30 μM of LY204002 or 20 μM of PP2 for 0.5 h. The cells were stained with 5 μM of BES-H_2O_2. ROS production was measured using flow cytometry. (D) siRNA-treated HepG2 cells were subjected to immunoblotting analyses using OSSA antibody. (E) Immunoblotting analyses of HepG2 cells transfected with a non-targeting siRNA or two separate OSSA siRNAs in the absence or presence of 5.5 mM of glucose for the indicated times. (F) Addition of H_2O_2 to the medium of OSSA-knockdown cells containing 5.5 mM glucose for 0.5 h, followed by immunoblotting.
doi:10.1371/journal.pone.0056628.g003

knockdown of NOX5 did not alter the AKT phosphorylation level (Fig. S10A, B).

Discussion

In this study, we tried to elucidate the mechanism of sensing of the extracellular glucose concentration by cells, using AKT phosphorylation as a marker. As reported previously, AKT phosphorylation is induced by glucose deprivation [9,10]. In addition, increase in AKT phosphorylation has also been confirmed in HepG2 cells cultured in media containing one-quarter of the normal physiological glucose concentration. This fact suggests that cells have sophisticated mechanisms for monitoring extracellular glucose levels. In another study, increase in AKT phosphorylation was confirmed in PANC-1 cells cultured in the presence of glucose levels that are one-eighth of the normal physiological condition. The difference in the minimal trigger concentration of glucose between the HepG2 cells and PANC-1 cells could be related to differences in the origins of the cells or differences in the microenvironments of the tumors the cells were derived from.

In the present study, increase in ROS production was observed by 30 minutes after glucose deprivation, both in cancer cells and human fibroblasts. Thus, it became evident that the mechanism of ROS production under glucose deprivation is preserved in not only cancer cells, but also human fibroblasts. ROS was strongly suspected to mediate the AKT phosphorylation, because AKT

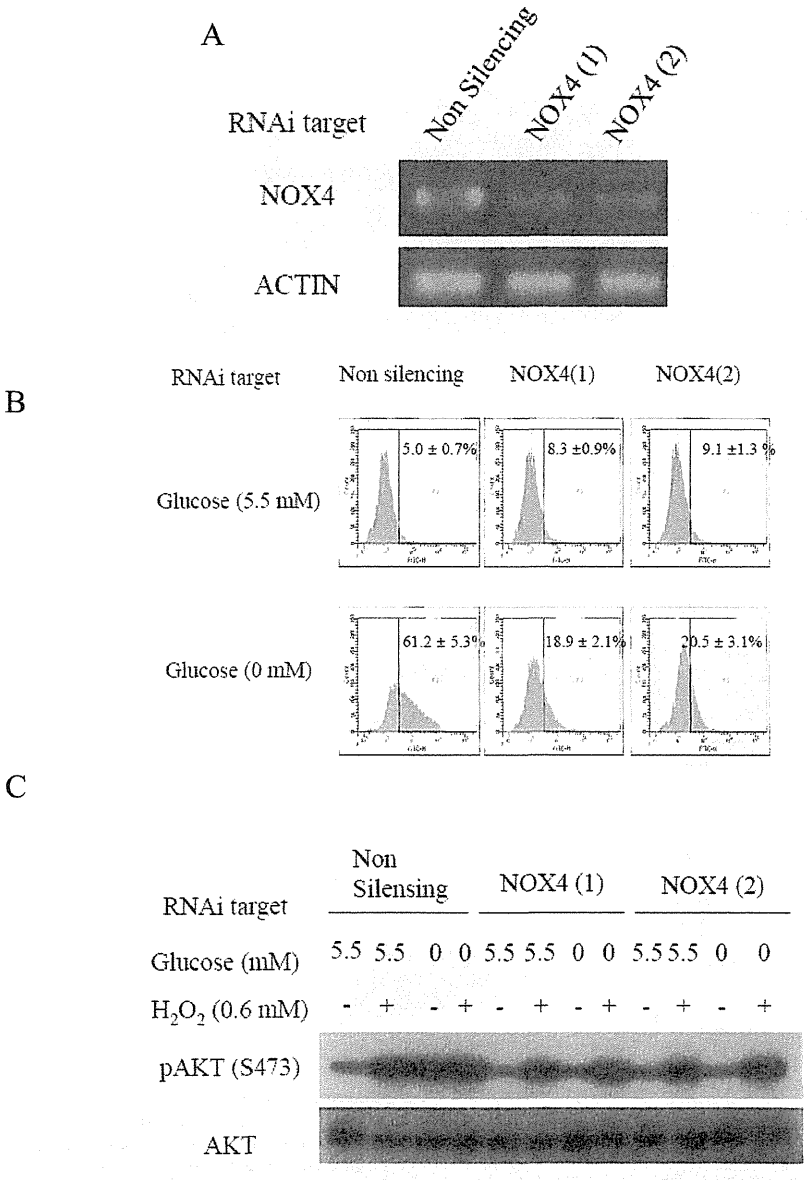

Figure 4. Induction of AKT phosphorylation under glucose deprivation is mediated by ROS generated by NOX4. (A) siRNA-treated HepG2 cells were subjected to reverse-transcriptase PCR (RT-PCR) to confirm NOX4 knockdown. (B) NOX4 knockdown HepG2 Cells were stained with 5 μM of BES-H_2O_2 in the absence or presence of 5.5 mM of glucose for 0.5 h. ROS production was measured using flow cytometry. (C) Immunoblotting analyses of HepG2 cells transfected with a non-targeting siRNA or two separate NOX4 siRNAs in the absence or presence of 5.5 mM of glucose or treatment with exogenous H_2O_2 for 0.5 h.
doi:10.1371/journal.pone.0056628.g004

phosphorylation was inhibited by treatment with NAC. As H_2O_2 has a low selectivity for downstream molecules, it may be involved in the regulation of numerous signaling pathways [27,28,29]. Among them, the regulation of AKT phosphorylation, as reported here, is particularly intriguing. AKT mediates cell proliferation and survival [30,31]. In our previous work, Akt activation was found to play a critical role in cell survival under glucose deprivation [10]. Furthermore, OSSA knockdown and the inhibition of SRC by PP2 suggests that these two elements are fundamental to AKT phosphorylation induced by glucose deprivation. It has been reported that SRC family kinases as their redox sensitive cysteines are the targets of specific oxidation by various oxidants, including H_2O_2 [32]. In this study, we clarified that PP2, a specific SRC inhibitor, inhibited AKT phosphorylation induced by glucose deprivation and exogeneous hydrogen peroxide. Thus, SRC is a strong candidate as a hydrogen peroxide sensor. Since PP2 inhibits SRC and other members of the SRC family, we should be careful before denying the relevance of other SRC family kinases [25]. Further investigations, such as by knockdown of individual SRC family kinases will be needed to identify the relevant Src-family kinase.

As with most intracellular signaling cascades, cross-talk and feedback interactions contribute to the overall regulation of PI3K/AKT signaling. S6 kinase-1, a downstream effector of mTORC1,

is known to be involved in a negative feedback loop of AKT activation. S6 kinase phosphorylates and inhibits upstream insulin receptor substrate proteins, which diminishes signaling through the PI3K/AKT pathway [33]. We observed that S6 kinase-1 phosphorylation was suppressed in PANC-1 cells under glucose deprivation (unpublished data), suggesting that the negative feedback machinery could be another mechanism regulating AKT phophorylation in cells under glucose deprivation. Furthermore, it was considered that the NADPH/NADP and ATP/AMP ratios may possibly change under glucose deprivation. Therefore, we measured the NADPH/NADP and ATP/AMP ratios; however, no significant changes were observed in at least the first 30 minutes. We also examined the effect of AMPK activation induced by AICAR on AKT activation and the cellular levels of hydrogen peroxide level, but again no significant changes were observed (unpublished data).

AKT phosphorylation in response to glucose deprivation was also completely inhibited following the addition of galactose or fructose instead of glucose. Galactose and fructose enter the glycolytic pathway after they have been metabolized intracellularly to glucose-6-phosphate and fructose-1 or 6-phosphate, respectively. Therefore, the contribution of decrease in metabolites downstream of fructose-1 or 6-phosphate to the induction of AKT phosphorylation under glucose deprivation was hypothesized.

To examine the contribution of the mitochondria, which are the major loci of ROS production, PANC-1 Rho^0 cells depleted of mitochondrial DNA were produced. When the Rho^0 cells were exposed to glucose-deprived medium, a large amount of intracellular H_2O_2 was produced. As pyruvic acid alone did not inhibit the ROS production completely, we could not assess the contribution of the mitochondria to the induction of ROS production by glucose deprivation further by this method (Shimoda et al. unpublished data). We then studied the involvement of NOX4 as another major locus of ROS production. AKT phosphorylation induced by glucose deprivation was not observed after NOX4 knockdown; no increase in the intracellular ROS levels was observed either, indicating the involvement of NOX4 in the intracellular accumulation of ROS. The contribution of NOX4, but not NOX5, in the signaling triggered by glucose deprivation was rather unexpected. Interestingly, a previous study reported that NOX4 regulates the survival of PANC-1 cells via ROS/ASK1/AKT signaling [34]. It might also be involved in cell survival under glucose-deprived conditions. With respect to the regulation of their activities, there are fundamental differences among the NOX isoforms. Most NOX family members are reportedly switched on and off by their regulatory subunits. NOX4 also functions as a complex with p22phox on internal membranes to produce ROS [35,36]. NOX4, unlike other members of the NOX family, is known to constitutively induce the production of large amounts of H_2O_2, however, the possibility of growth factor signaling being mediated by NOX4 has also been suggested [37]. The results of the present study also suggested that the activity of NOX4 might be regulated. In the present study, glucose deprivation increased the cellular levels of H_2O_2, which was suppressed by frucotose and galactose, indicating that NOX4 might be activated by deprivation of some glycolytic intermediate or some downstream products, such as of the pentose phosphate shunt and/or TCA cycle. The results obtained with the use of 2-DG are consistent with this idea. Whether the ROS accumulation under glucose deprivation is caused by increased production of ROS as a result of enhanced activity of NOX4, or by decreased antioxidant capacity, such as that associated with deficient activities of catalase, glutathione peroxidase, and glutathione needs to be further investigated. The intracellular amount of ROS is determined by the activity of the enzymes and the amounts of the substrates available. Therefore, metabolomic analysis of the entire set of metabolites is desired.

In the present study, we found that cells sense and respond to metabolic flux rather than glucose itself, and NOX4 and its product, ROS, play important roles in the cellular adaptive responses.

Supporting Information

Figure S1 Immunoblotting analyses after incubating PANC-1 cells in the absence or presence of 5.5 mM of glucose in the absence or presence of 30 μM of LY294002 for the indicated times.
(TIF)

Figure S2 Immunoblotting analyses after incubating human fibroblasts derived from subserossa of stomach in the absence or presence of 5.5 mM of glucose for 0.5 h.
(TIF)

Figure S3 PANC-1 cells were treated with or without various concentrations of glucose for 0.5 h.
(TIF)

Figure S4 Immunoblotting analyses after incubating PANC-1 cells in the absence or presence of 5.5 mM of glucose, 5.5 mM of galactose, or 5.5 mM of fructose for 0.5 h.
(TIF)

Figure S5 PANC-1 cells were cultured in either glucose-containing medium or glucose-deprived medium for 0.5 h. Cells were stained with 5 μM BES-H_2O_2. ROS production was measured using flow cytometry.
(TIF)

Figure S6 Human fibroblasts derived from subserossa of stomach were cultured in either glucose-containing medium or glucose-deprived medium for 0.5 h. Cells were stained with 5 μM BES-H_2O_2. ROS production was measured using flow cytometry.
(TIF)

Figure S7 HepG2 cells were cultured in the absence or presence of 5.5 mM of glucose, 5.5 mM of galactose, or 5.5 mM of fructose for 0.5 h. ROS production was measured using flowcytometry. Cells were stained with 5 μM of BES-H_2O_2.
(TIF)

Figure S8 Immunoblotting analyses of HepG2 cells in the absence or presence of 5.5 mM of glucose or treatment with exogenous H_2O_2 for 0.5 h.
(TIF)

Figure S9 (A) siRNA-treated PANC-1 cells were subjected to reverse transcriptional PCR (RT-PCR) to confirm NOX4 knockdown. (B) Immunoblotting analyses after incubating PANC-1 cells transfected with a non-targeting siRNA or two separate NOX4 siRNA in the absence or presence of 5.5 mM of glucose for 0.5 h.
(TIF)

Figure S10 (A) siRNA-treated PANC-1 cells were subjected to reverse transcriptional PCR (RT-PCR) to confirm NOX5 knockdown. (B) Immunoblotting analyses after incubating

PANC-1 cells transfected with a non-targeting siRNA or two separate NOX5 siRNA in the absence or presence of 5.5 mM of glucose for 0.5 h.
(TIF)

Acknowledgments

We thank Dr. Ryuichi Sakai (National Cancer Center Research Institute) for kindly gifting the OSSA antibody.

We thank Dr. Atsushi Ochiai (Pathology Division, Research Center for Innovative Oncology, National Cancer Center Hospital East) for kindly gifting the primary human stomach subserosal fibroblasts.

Author Contributions

Conceived and designed the experiments: SO HE KT. Performed the experiments: SO YS. Analyzed the data: SO YS. Wrote the paper: SO HE KT.

References

1. Flick KM, Spielewoy N, Kalashnikova TI, Guaderrama M, Zhu QZ, et al. (2003) Grr1-dependent inactivation of Mth1 mediates glucose-induced dissociation of Rgt1 from HXT gene promoters. Mol Biol Cell 14: 3230–3241.
2. Kim JH, Polish J, Johnston M (2003) Specificity and regulation of DNA binding by the yeast glucose transporter gene repressor Rgt1. Mol Cell Biol 23: 5208–5216.
3. Ozcan S, Johnston M (1999) Function and regulation of yeast hexose transporters. Microbiol Rev 63: 554–569.
4. Brown JM, Giaccia AJ (1998) The unique physiology of solid tumors: Opportunities (and problems) for cancer therapy. Cancer Res 58: 1408–1416.
5. Jain RK (2003) Molecular regulation of vessel maturation. Nat Med 9: 685–693.
6. Less JR, Skalak TC, Sevick EM, Jain RK (1991) Microvascular Architecture in a Mammary-Carcinoma - Branching Patterns and Vessel Dimensions. Cancer Res 51: 265–273.
7. Thomlinson RH, Gray LH (1955) The histological structure of some human lung cancers and the possible implications for radiotherapy. Br J Cancer 9: 539–49.
8. Hirayama A, Kami K, Sugimoto M, Sugawara M, Toki N, et al. (2009) Quantitative Metabolome Profiling of Colon and Stomach Cancer Microenvironment by Capillary Electrophoresis Time-of-Flight Mass Spectrometry. Cancer Res 69: 4918–4925.
9. Esumi H, Lu J, Kurashima Y, Hanaoka T (2004) Antitumor activity of pyrvinium pamoate, 6-(dimethylamino)-2- 2-(2,5-dimethyl-1-phenyl-1H- pyrrol-3-yl)ethenyl -1-methyl-quinolinium pamoate salt, showing preferential cytotoxicity during glucose starvation. Cancer Sci 95: 685–690.
10. Izuishi K, Kato K, Ogura T, Kinoshita T, Esumi H (2000) Remarkable tolerance of tumor cells to nutrient deprivation: Possible new biochemical target for cancer therapy. Cancer Res 60: 6201–+.
11. Alvarez-Tejado M, Alfranca A, Aragones J, Vara A, Landazuri MO, et al. (2002) Lack of evidence for the involvement of the phosphoinositide 3-kinase/Akt pathway in the activation of hypoxia-inducible factors by low oxygen tension. J Biol Chem 277: 13508–13517.
12. Bang OS, Ha BG, Park EK, Kang SS (2000) Activation of Akt is induced by heat shock and involved in suppression of heat-shock-induced apoptosis of NIH3T3 cells. Biochem Biophys Res Commun 278: 306–311.
13. Esposito F, Chirico G, Gesualdi NM, Posadas I, Ammendola R, et al. (2003) Protein kinase B activation by reactive oxygen species is independent of tyrosine kinase receptor phosphorylation and requires Src activity. J Biol Chem 278: 20828–20834.
14. Jiang ZJ, Zhang Y, Chen XQ, Lam PY, Yang H, et al. (2002) Activation of Erk1/2 and Akt in astrocytes under ischemia. Biochem Biophys Res Commun 294: 726–733.
15. Nomura M, Kaji A, Ma WY, Zhong SP, Liu GM, et al. (2001) Mitogen and stress-activated protein kinase 1 mediates activation of Akt by ultraviolet B irradiation. J Biol Chem 276: 25558–25567.
16. Tomitsuka E, Kita K, Esumi H (2012) An anticancer agent, pyrvinium pamoate inhibits the NADH-fumarate reductase system–a unique mitochondrial energy metabolism in tumour microenvironments. J Biochem 152: 171–83.
17. Inazuka F, Sugiyama N, Tomita M, Abe T, Shioi G, et al. (2012) Muscle-specific Knock-out of NUAK Family SNF1-like Kinase 1 (NUAK1) Prevents High Fat Diet-induced Glucose Intolerance. J Biol Chem 287: 16379–16389.
18. Guo M, Joiakim A, Reiners JJ (2000) Suppression of 2,3,7,8-tetrachlorodibenzo-p-dioxin (TCDD)-mediated aryl hydrocarbon receptor transformation and CYP1A1 induction by the phosphatidylinositol 3-kinase inhibitor 2-(4-morpholinyl)-8-phenyl-4H-1-benzopyran-4-one (LY294002). Biochemical Pharmacol 60: 635–642.
19. Crane RK, Sols A (1954) The non-competitive inhibition of brain hexokinase by glucose-6-phosphate and related compounds. J Biol Chem 210: 597–606.
20. Tower DB (1958) The effects of 2-deoxy-D-glucose on metabolism of slices of cerebral cortex incubated in vitro. J Neurochem 3: 185–205.
21. Liu L, Wise DR, Diehl JA, Simon MC (2008) Hypoxic Reactive Oxygen Species Regulate the Integrated Stress Response and Cell Survival. J Biol Chem 283: 31153–31162.
22. Bensaad K, Cheung EC, Vousden KH (2009) Modulation of intracellular ROS levels by TIGAR controls autophagy. EMBO J 28: 3015–3026.
23. Maeda H, Futkuyasu Y, Yoshida S, Fukuda M, Saeki K, et al. (2004) Fluorescent probes for hydrogen peroxide based on a non-oxidative mechanism. Angew Chem Int Ed 43: 2389–2391.
24. Tanaka M, Sasaki K, Kamata R, Hoshino Y, Yanagihara K, et al. (2009) A Novel RNA-Binding Protein, Ossa/C9orf10, Regulates Activity of Src Kinases To Protect Cells from Oxidative Stress-Induced Apoptosis. Mol Cell Biol 29: 402–413.
25. Hanke JH, Gardner JP, Dow RL, Changelian PS, Brissette WH, et al. (1996) Discovery of a novel, potent, and Src family-selective tyrosine kinase inhibitor - Study of Lck- and FynT-dependent T cell activation. J Biol Chem 271: 695–701.
26. Xi G, Shen X, Maile LA, Wai C, Gollahon K, et al. (2012) Hyperglycemia Enhances IGF-I-Stimulated Src Activation via Increasing Nox4-Derived Reactive Oxygen Species in a PKC zeta-Dependent Manner in Vascular Smooth Muscle Cells. Diabetes 61: 104–113.
27. Aggeli I-KS, Gaitanaki C, Beis I (2006) Involvement of JNKs and p38-MAPK/MSK1 pathways in H2O2-induced upregulation of heme oxygenase-1 mRNA in H9c2 cells. Cell Signal 18: 1801–1812.
28. Kim YK, Bae GU, Kang JK, Park JW, Lee EK, et al. (2006) Cooperation of H2O2-mediated ERK activation with Smad pathway in TGF-beta 1 induction of p21(WAF1/Cip1). Cell Signal 18: 236–243.
29. Takada Y, Mukhopadhyay A, Kundu GC, Mahabeleshwar GH, Singh S, et al. (2003) Hydrogen peroxide activates NF-kappa B through tyrosine phosphorylation of I kappa B alpha and serine phosphorylation of p65 - Evidence for the involvement of I kappa B alpha kinase and Syk protein-tyrosine kinase. J Biol Chem 278: 24233–24241.
30. Burgering BMT, Coffer PJ (1995) Protein-Kinase-B (C-Akt) In Phosphatidylinositol-3-Oh Inase Signal-Transduction. Nature 376: 599–602.
31. Franke TF, Yang SI, Chan TO, Datta K, Kazlauskas A, et al. (1995) The Protein-Kinase Encoded by the Akt Protooncogene Is a Target of the Pdgf-Activated Phosphatidylinositol 3-Kinase. Cell 81: 727–736.
32. Giannoni E, Buricchi F, Raugei G, Ramponi G, Chiarugi P (2005) Intracellular reactive oxygen species activate Src tyrosine kinase during cell adhesion and anchorage-dependent cell growth. Mol Cell Biol 25: 6391–6403.
33. Tremblay F, Brule S, Um SH, Li Y, Masuda K, et al. (2007) Identification of IRS-1 Ser-1101 as a target of S6K1 in nutrient- and obesity-induced insulin resistance. Proc Natl Acad Sci U S A 104: 14056–14061.
34. Mochizuki T, Furuta S, Mitsushita J, Shang W, Ito M, et al. (2006) Inhibition of NADPH oxidase 4 activates apoptosis via the AKT/apoptosis signal-regulating kinase 1 pathway in pancreatic cancer PANC-1 cells. Oncogene 25: 3699–3707.
35. Sumimoto H, Miyano K, Takeya R (2005) Molecular composition and regulation of the Nox family NAD(P)H oxidases. Biochem Biophys Res Commun 338: 677–686.
36. Martyn KD, Frederick LM, von Loehneysen K, Dinauer MC, Knaus UG (2006) Functional analysis of Nox4 reveals unique characteristics compared to other NADPH oxidases. Cell Signal 18: 69–82.
37. Kim HJ, Kim C-H, Ryu J-H, Joo JH, Lee S-N, et al. (2011) Crosstalk between platelet-derived growth factor-induced Nox4 activation and MUC8 gene overexpression in human airway epithelial cells. Free Radic Biol Med 50: 1039–1052.

Drug Design, Development and Therapy Dove

ORIGINAL RESEARCH

(+)-Grandifloracin, an antiausterity agent, induces autophagic PANC-1 pancreatic cancer cell death

Jun-ya Ueda[1,2]
Sirivan Athikomkulchai[3]
Ryuta Miyatake[4]
Ikuo Saiki[2]
Hiroyasu Esumi[5,6]
Suresh Awale[1,2]

[1]Frontier Research Core for Life Sciences, [2]Institute of Natural Medicine, University of Toyama, Toyama, Japan; [3]Faculty of Pharmacy, Srinakharinwirot University, Nakhon Nayok, Thailand; [4]Graduate School of Science and Engineering, University of Toyama, Toyama, Japan; [5]Research Institute for Biomedical Sciences, Tokyo University of Science, [6]National Cancer Center Hospital East, Chiba, Japan

Abstract: Human pancreatic tumors are known to be highly resistant to nutrient starvation, and this prolongs their survival in the hypovascular (austere) tumor microenvironment. Agents that retard this tolerance to nutrient starvation represent a novel antiausterity strategy in anticancer drug discovery. (+)-Grandifloracin (GF), isolated from *Uvaria dac*, has shown preferential toxicity to PANC-1 human pancreatic cancer cells under nutrient starvation, with a PC_{50} value of 14.5 μM. However, the underlying mechanism is not clear. In this study, GF was found to preferentially induce PANC-1 cell death in a nutrient-deprived medium via hyperactivation of autophagy, as evidenced by a dramatic upregulation of microtubule-associated protein 1 light chain 3. No change was observed in expression of the caspase-3 and Bcl-2 apoptosis marker proteins. GF was also found to strongly inhibit the activation of Akt, a key regulator of cancer cell survival and proliferation. Because pancreatic tumors are highly resistant to current therapies that induce apoptosis, the alternative cell death mechanism exhibited by GF provides a novel therapeutic insight into antiausterity drug candidates.

Keywords: (+)-grandifloracin, antiausterity strategy, PANC-1, nutrient starvation

Introduction

Human pancreatic cancer is the most fatal form of cancer worldwide, with a 5-year survival rate of less than 5%.[1] Each year, approximately 29,000 people are diagnosed with pancreatic cancer in Japan.[2] The annual mortality rate from this malignancy closely approximates the annual incidence rate.[3,4] Once diagnosed, the average life expectancy is 6 months. It is the fifth leading cause of cancer-related mortality in Japan and other industrialized countries.[4] Until now, no effective treatment has been available.[5,6] Human pancreatic cancer shows resistance to most conventional chemotherapeutic drugs in clinical use, such as paclitaxel, doxorubicin, and cisplatin.[7] At present, gemcitabine and S-1 (tegafur + gimeracil + oteracil potassium) are the only standard regimens for advanced pancreatic cancer.[8–11] Therefore, effective chemotherapeutic agents against this disease are urgently needed. Human pancreatic tumors are hypovascular in nature,[12] causing a limited supply of nutrients and oxygen to reach the aggressively proliferating tumor cells.[13] As tumor cells proliferate, the demand for essential nutrients and oxygen exceeds the supply. Consequently, large areas of tumor survive under the hostile environment characterized by nutrient and oxygen starvation. Yet, human pancreatic tumor cells show the extraordinary ability to tolerate such extreme states through the modulation of energy metabolism.[14] While normal human cells die within 24 hours under nutrient starvation, some human pancreatic cancer cell lines can survive up to 72 hours in the complete absence of nutrients such as glucose, amino acids, and serum.[14]

Correspondence: Suresh Awale
Frontier Research Core for Life Sciences, University of Toyama, 2630 Sugitani, Toyama 930-0194, Japan
Tel +81 76 434 7640
Fax +81 76 434 7640
Email suresh@inm.u-toyama.ac.jp

This remarkable tolerance to nutrient starvation is one of the key factors for survival and progression of pancreatic tumors. Therefore, agents that retard the tolerance of cancer cells to nutrient starvation represent a novel approach in anticancer drug discovery.[15] Using this hypothesis, we established a novel antiausterity strategy for the discovery of anticancer agents that preferentially target tolerance to nutrient starvation by cancer cells. Previous work on this strategy has led to the discovery of a number of potent anticancer agents, such as arctigenin,[15] angelmarin,[16] kayeassamins A–I,[17,18] and panduratins,[19,20] from the medicinal plants used in Japanese Kampo medicine and Southeast Asian countries.[21] Interestingly, these compounds also strongly suppressed tumor growth in a xenograft model using pancreatic cancer cells.[15] In our continued work, we recently found that a dichloromethane extract of the stem of *Uvaria dac* preferentially inhibited PANC-1 human pancreatic cancer cell survival under nutrient deprivation.[22] Work-up of this bioactive extract led to the discovery of (+)-grandifloracin (GF) as a potent antiausterity agent that showed preferential toxicity to PANC-1 cells with a PC_{50} value of 14.5 μM. In this study, we explored the underlying mechanism of GF-induced modulation of key regulatory proteins involved in tolerance to nutrient starvation in PANC-1 cells.

Materials and methods

Reagents

GF (Figure 1) was isolated from the stems of *U. dac* as described previously.[22] GF purity was determined to be 95% by high-performance liquid chromatography. Conventional anticancer agents, ie, gemcitabine, 5-fluorouracil, 2-deoxyglucose, paclitaxel, podophyllotoxin, and camptothecin, were purchased from Sigma-Aldrich (St Louis, MO, USA). Each reagent was dissolved in dimethyl sulfoxide as a 10 mM stock solution and stored at −30°C until use. Dilution to give the desired concentration was performed prior to treatment. Dulbecco's phosphate-buffered saline was purchased from Nissui Pharmaceutical (Tokyo, Japan). Dulbecco's Modified Eagle's Medium. (DMEM) was purchased from Wako Pure Chemical (Osaka, Japan). Sodium bicarbonate, potassium chloride, magnesium sulfate, sodium dihydrogen phosphate, potassium dihydrogen phosphate, sodium chloride, and phenol red were purchased from Wako Pure Chemical. HEPES was purchased from Dojindo Laboratories (Kumamoto, Japan). Fetal bovine serum was purchased from Nichirei Biosciences Inc. (Tokyo, Japan). Antibiotic/antimycotic solution was purchased from Sigma-Aldrich. The WST-8 cell counting kit was purchased from Dojindo Laboratories. Cell culture flasks and 96-well plates were obtained from Falcon Becton Dickinson Labware (BD Biosciences, San Jose, CA, USA). Nutrient-deprived medium was prepared according to a previously described protocol.[14] Rabbit polyclonal antibodies to Akt, phosphoryl Akt (Ser473), mammalian target of rapamycin (mTOR), phosphoryl mTOR (Ser2448), Bcl-2, caspase 3, and LC3A/B were purchased from Cell Signaling Technology (Danvers, MA, USA). A goat polyclonal antibody to actin was purchased from Santa Cruz Biotechnologies (Dallas, TX, USA). Horseradish peroxidase-conjugated goat polyclonal anti-rabbit and rabbit polyclonal anti-goat immunoglobulins were purchased from DakoCytomation (Glostrup, Denmark).

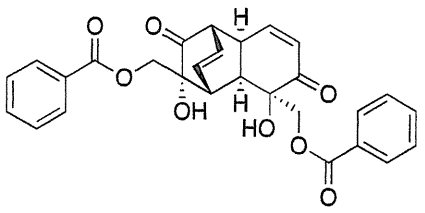

Figure 1 Chemical structure of (+)-grandifloracin.

Cell line

The PANC-1 (RBRC-RCB2095) cell line was purchased from the Riken BRC Cell Bank (Ibaraki, Japan) and maintained in standard DMEM with 10% fetal bovine serum supplement, 100 U/mL of penicillin G, 0.1 mg/mL of streptomycin, and 0.25 μg/mL of amphotericin B.

Preferential cytotoxic activity

The in vitro preferential cytotoxicity of GF was determined using a previously described procedure with a slight modification.[22] In brief, human pancreatic cancer cells were seeded in 96-well plates (1.5×10^4/well) and incubated in fresh DMEM at 37°C under humidified 5% CO_2 and 95% air for 24 hours. After the cells were washed with Dulbecco's phosphate-buffered saline, the medium was changed to serially diluted test samples in DMEM or nutrient-deprived medium, with the control and blank in each plate. After 24 hours of incubation, 100 μL of DMEM containing 10% WST-8 cell counting kit solution was directly added to each well. After 3 hours of incubation, absorbance at 450 nm was measured (EnSpire® Multilabel Reader, PerkinElmer, Waltham, MA, USA). Cell viability was calculated from the mean values for three wells using the following equation:

$$\text{Cell viability (\%)} = [(\text{Abs}_{(\text{test sample})} - \text{Abs}_{(\text{blank})})/(\text{Abs}_{(\text{control})} - \text{Abs}_{(\text{blank})})] \times 100$$

Morphologic assessment

Cells were seeded in 60 mm dishes (1×10^6 cells) and incubated in a humidified CO_2 incubator for 24 hours to allow cell attachment. The cells were then washed twice with Dulbecco's phosphate-buffered saline and treated with 25 μM GF in DMEM, nutrient-deprived medium, and the control. After 12 and 24 hours of incubation, the cells were treated with fluorescein-labeled annexin V and propidium iodide, and cell morphology was observed using an inverted Nikon Eclipse TS 100 microscope (40× objective) with phase-contrast and fluorescence modes. Microscopic images were taken using a Nikon DS-L-2 camera directly attached to the microscope.

Annexin V/dead cell assay

The annexin V/dead cell assay was performed in a Muse™ cell analyzer (Merck Millipore, Billerica, MA, USA) utilizing a Muse annexin V and dead cell kit. The assay utilizes phycoerythrin-labeled annexin V to detect phosphatidylserine on the external membrane of apoptotic cells. The kit contains the DNA dye, 7-aminoactinomycin D (7-AAD) for the exclusion of nonviable cells. Four populations of cells can be distinguished in this assay: nonapoptotic cells, annexin V (–) and 7-AAD (–); early apoptotic cells, annexin V (+) and 7-AAD (–); late-stage apoptotic and dead cells, annexin V (+) and 7-AAD (+); and necrotic nuclear debris, annexin V (–) and 7-AAD (+). The assay was performed according to the manufacturer's protocol. In brief, the cells were seeded in 60 mm dishes (1×10^6 cells) and incubated in a humidified CO_2 incubator for 24 hours to allow cell attachment. The cells were then washed twice with Dulbecco's phosphate-buffered saline and treated with 12.5 μM GF, 25 μM GF, or the control of nutrient-deprived medium for the indicated time periods. The cells were then harvested from the dish with trypsin to give single cell suspensions. Finally, 100 μL of annexin V/dead reagent and 100 μL of a single cell suspension were mixed in a microtube and incubated for 20 minutes at room temperature in the dark. The cells were then analyzed using the Muse cell analyzer, and 5,000 cell events were collected for each sample. The images were acquired as the screenshots of the processed data and the text size was edited for clarity.

Western blot analysis

Proteins were separated by gel electrophoresis on a polyacrylamide gel containing 0.1% sodium dodecyl sulfate and transferred to polyvinylidene fluoride membranes. The membranes were blocked with Block Ace® (DS Pharma Medical, Suita, Japan), washed with Dulbecco's phosphate-buffered saline containing 0.1% polyoxyethylene (20) sorbitan monolaurate (Wako Pure Chemical), and incubated overnight with primary antibodies diluted in Can Get Signal® (Toyobo, Osaka, Japan). After washing, the membranes were incubated for 45 minutes at room temperature with horseradish peroxidase-conjugated anti-rabbit or anti-goat immunoglobulins as the secondary antibody. The bands were detected with an enhanced chemiluminescence solution (PerkinElmer). The images were analyzed using Image Studio software version 3.1.4.

Statistical analysis

Statistical analysis was performed using the unpaired Student's *t*-test. A P-value<0.05 was considered to be statistically significant.

Results

GF showed preferential cytotoxicity in a concentration-dependent manner

The PANC-1 cell line is highly resistant to nutrient deprivation and shows an extraordinary ability to survive for >48 hours even under complete nutrient starvation. GF remarkably diminished tolerance to nutrient starvation in a concentration-dependent manner (Figure 2A). Cells exposed to GF at 25 μM showed 100% cell death within 24 hours in nutrient-deprived medium, with a PC_{50} value of 14.5 μM; however, no toxicity was observed in nutrient-rich DMEM.

GF sensitized PANC-1 cell death under glucose/serum-deprived conditions

To determine the conditions under which GF induces sensitivity to nutrient starvation resulting in cell death, the PANC-1 cells were treated with 25 μM GF under various nutrient conditions of glucose, amino acids, and serum. Cell viability was measured 24 hours after treatment. As shown in Figure 2B, GF was found to be toxic during glucose or serum deprivation, irrespective of the presence or absence of amino acids. In the presence of glucose and serum, cell viability was 100%. However, removal of serum led to a decrease in cell viability to 73% and 69% in the presence or absence of amino acids, respectively. Similarly, removal of glucose also led to a significant decrease in cell viability to 66%. Removal of both glucose and serum decreased cell viability to 2%.

Conventional anticancer agents are ineffective against PANC-1 cells in nutrient-deprived medium

The preferential cytotoxicity of GF was compared with that of several conventional anticancer agents, including

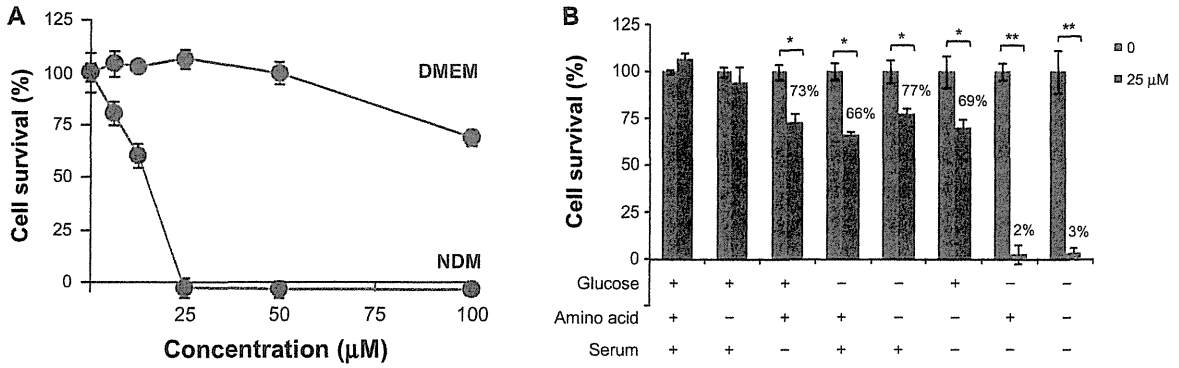

Figure 2 Effect of (+)-grandifloracin on PANC-1 cell survival after 24 hours in NDM and normal medium (DMEM). (**A**) Effect of (+)-grandifloracin concentration on cell survival in NDM and DMEM. (**B**) Effects of medium components, ie, glucose, amino acids, and serum. Data are expressed as the mean ± standard deviation, n=3. *$P<0.05$; **$P<0.01$ indicate significant difference from the control.
Abbreviations: NDM, nutrient-deprived medium; DMEM, Dulbecco's Modified Eagle's Medium.

gemcitabine, 5-fluorouracil, 2-deoxyglucose, paclitaxel, camptothecin, and podophyllotoxin, using PANC-1 cells grown in nutrient-deprived medium versus DMEM (Figure 3). All tested agents were virtually inactive in nutrient-deprived medium; however, paclitaxel and camptothecin showed weak activity in nutrient-rich DMEM at the maximum tested dose of 100 μM after 24 hours. Because some of the conventional anticancer agents showed weak activity in DMEM, their effects during prolonged treatment were also evaluated by monitoring their cytotoxicity after 24, 48, and 72 hours. As shown in Figure 4, gemcitabine and 5-fluorouracil weakly decreased cell viability 72 hours after treatment. However, these compounds did not show a clear concentration-dependent effect. 2-Deoxyglucose was completely inactive. Paclitaxel and podophyllotoxin were found to reduce cell viability after 72 hours, but the effect was not concentration-dependent. On the other hand, camptothecin exhibited strong activity with cell viability of <25% at 10 μM 48 hours after treatment.

Assessment of GF-induced apoptosis

To investigate whether GF-induced cell death in nutrient-deprived medium involves apoptosis, the cell morphology was examined. As shown in Figure 5, at 25 μM, GF induced a marked change in PANC-1 cell morphology within 8 hours. However, the cells lacked the classical signs of apoptosis, such as shrinkage or fragmentation into membrane-bound apoptotic bodies. Instead, swelling and rupture of cell membranes and disruption of cellular organelles appeared to be closer to a necrotic-type cell death. Staining with annexin V/propidium iodide reagent showed an increased population of cells containing Annexin V (green fluorescence) and propidium iodide (red fluorescence). Annexin V is a Ca^{2+}-dependent phospholipid-binding protein with

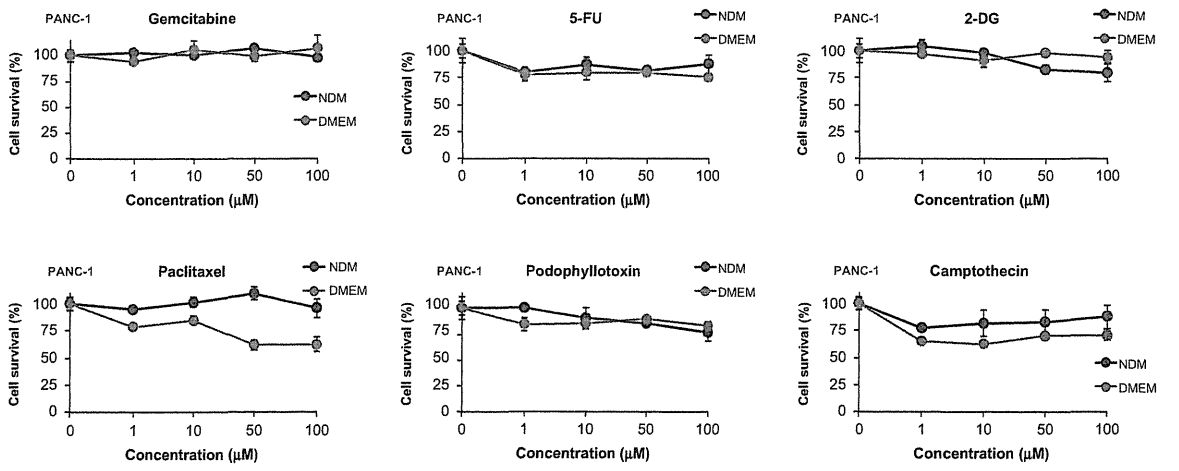

Figure 3 Effect of conventional anticancer agents against PANC-1 cells after 24 hours in NDM and DMEM. Data are expressed as the mean ± standard deviation, n=3.
Abbreviations: NDM, nutrient-deprived medium; DMEM, Dulbecco's Modified Eagle's Medium; 5-FU, 5-fluorouracil; 2-DG, 2-deoxyglucose.

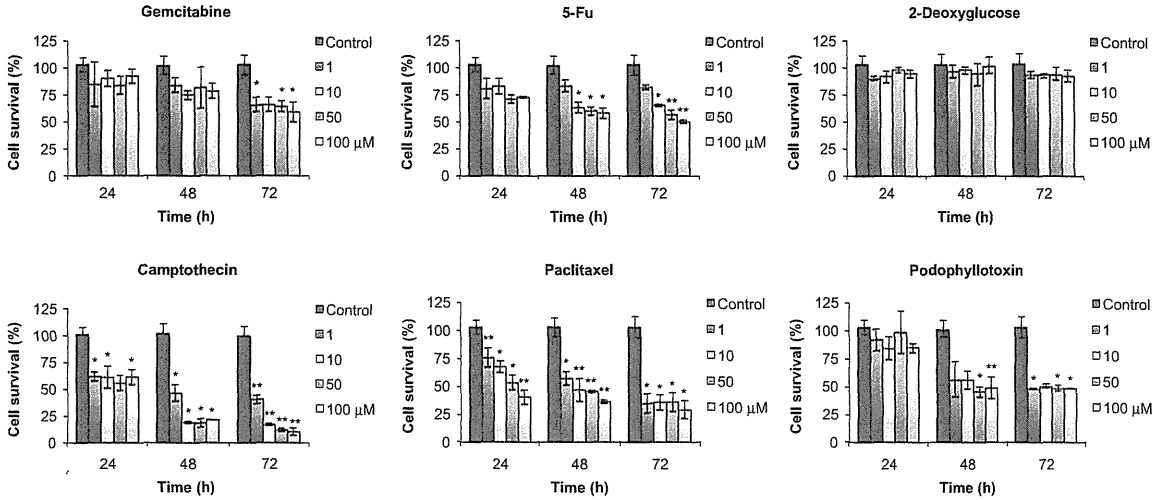

Figure 4 Assessment of cytotoxicity of conventional anticancer agents against PANC-1 cells in Dulbecco's Modified Eagle's Medium. Data are expressed as the mean ± standard deviation, n=3. *$P<0.05$; **$P<0.01$ indicates a significant difference from the control.
Abbreviation: 5-FU, 5-fluorouracil.

high affinity for phosphatidylserine. Translocation of phosphatidylserine to the external cell surface occurs both in apoptosis and necrosis. We further performed flow cytometric analysis of cells treated with GF utilizing the Muse Annexin V and dead cell kit, which contains 7-AAD as a dye for exclusion of nonviable cells. 7-AAD is impermeable to viable cells and does not stain viable or early apoptotic cells. In late apoptotic and necrotic cells, the integrity of the cell membrane decreases, which allows 7-AAD to pass through the membranes, intercalate into nucleic acids and DNA, and display red fluorescence. As shown in Figure 6, the cells are predominantly stained with both Annexin V and 7-AAD within 12 hours in a concentration-dependent manner. In the control of nutrient-deprived medium, more than 90% of the cells survived. After treatment with GF, this cell population decreased markedly to 72% (12.5 μM) and 29% (25 μM), with an increase in the late apoptotic/necrotic cell population from 1% (control) to 15% (12.5 μM) and 61% (25 μM), respectively (Figure 6). We further performed Western blot analysis to examine GF-induced apoptosis. Treatment with GF neither led to cleavage of caspase-3 nor showed Bcl-2 inhibition (data not shown).

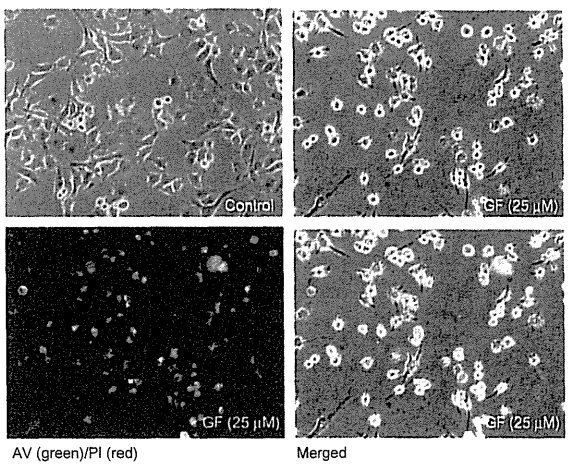

Figure 5 Effect of GF (25 μM) on PANC-1 cell morphology after 8 hours in NDM. Phase-contrast (upper left), fluorescent (lower left), and merged (lower right) images of PANC-1 cells.
Abbreviations: AV, Annexin V; PI, propidium iodide; NDM, nutrient-deprived medium; GF, (+)-grandifloracin.

GF inhibits Akt/mTOR activation

Akt is a prosurvival factor that is activated in a majority of tumors and regulates cellular functions such as cell cycle progression, cell migration, invasion, and angiogenesis. High Akt activation has been associated with tolerance to nutrient starvation and survival in an austerity environment.[14] Therefore, the effect of GF on Akt activation was investigated by Western blot analysis. As shown in Figure 6, Akt phosphorylation at Ser473 was completely inhibited by GF in a concentration-dependent as well as time-dependent manner in nutrient-deprived medium. GF also strongly suppressed total Akt. mTOR is a downstream effector of Akt and is frequently activated in various cancer types, where it is involved in tumor progression and metastasis.[23] Therefore, we tested whether GF has any modulatory activity against mTOR activation. As shown in Figure 7, addition of 25 μM GF completely inhibited mTOR phosphorylation at Ser2448 6 hours after treatment.

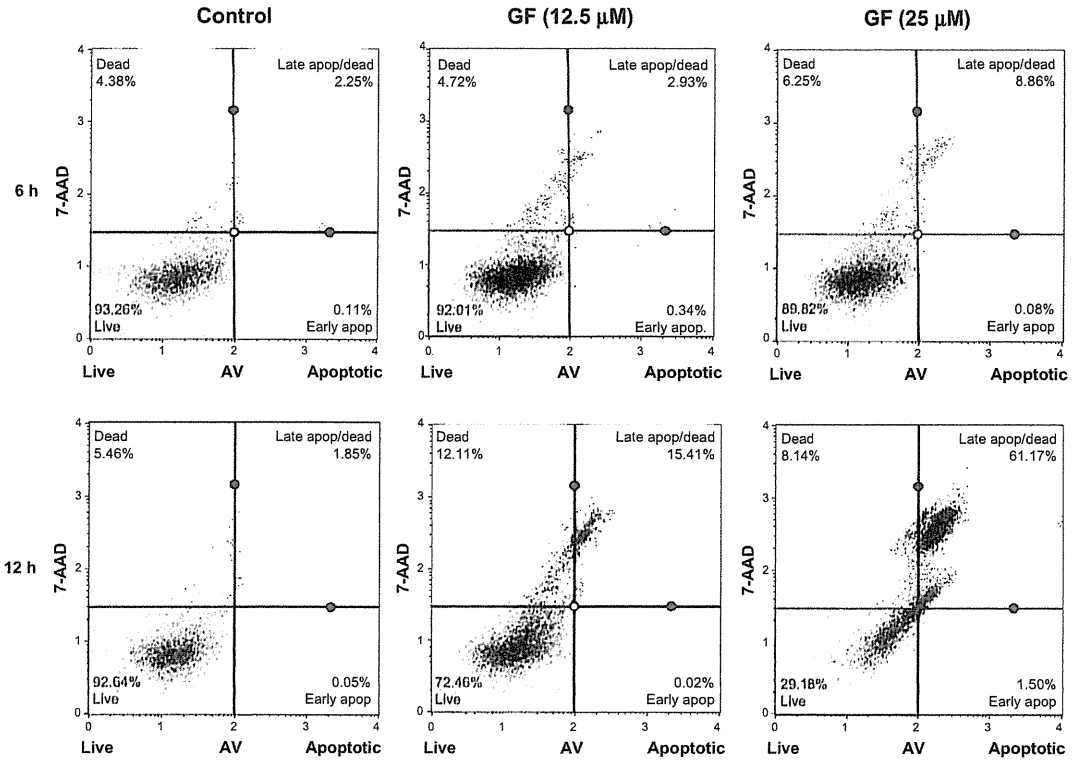

Figure 6 Assessment of apoptosis by GF. PANC-1 cells were treated with vehicle or GF (12.5 μM and 25 μM) in nutrient-deprived medium. After treatment (6 hours and 12 hours), the cells were treated with Annexin V/7-AAD reagent and cytometric analysis was performed.
Abbreviations: Apop, apoptotic; AV, Annexin V; GF, (+)-grandifloracin; 7-AAD; 7-aminoactinomycin D.

GF-induced autophagy in PANC-1 cells

Because no apoptotic cell death was observed in cells treated with GF, we speculated that GF might have induced autophagy. Therefore, expression of the autophagic marker microtubule-associated protein-light chain 3 (LC3), the cytoplasmic form of LC3-I (16 kDa), and the preautophagosomal and autophagosomal membrane-bound form of LC3-II (14 kDa) was examined by Western blot. The PANC-1 cells were cultured for varying time periods at different GF concentrations. As shown in Figure 7, no apparent differences were observed in LC3-I

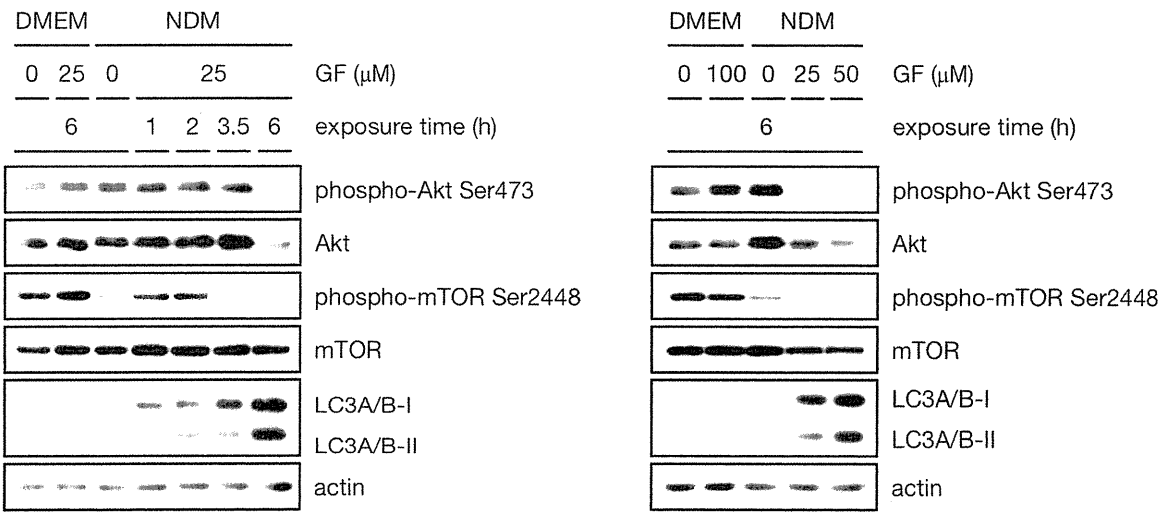

Figure 7 Effect of GF against Akt, mTOR, LC3A/B I, and LC3A/B II.
Abbreviations: GF, (+)-grandifloracin; NDM, nutrient-deprived medium; DMEM, Dulbecco's Modified Eagle's Medium.